July 2024

Fondazione Eni Enrico Mattei

Working Paper

18.2024

# A Hodrick-Prescott filter with automatically selected jumps

**Paolo Maranzano, Matteo Pelagatti**

# A Hodrick-Prescott filter with automatically selected jumps

**Paolo Maranzano** (Department of Economics, Management and Statistics, University of Milano-Bicocca and Fondazione Eni Enrico Mattei), **Matteo Pelagatti** (Department of Economics, Management and Statistics, University of Milano-Bicocca)

## Summary

The Hodrick-Prescott filter is a popular tool in macroeconomics for decomposing a time series into a smooth trend and a business cycle component. The last few years have witnessed global events, such as the Global Financial Crisis, the COVID-19 pandemic, and the war in Ukraine, that have had abrupt structural impacts on many economic time series. Moreover, new regulations and policy changes generally lead to similar behaviours. Thus, those events should be absorbed by the trend component of the trend-cycle decomposition, but the Hodrick-Prescott filter does not allow for jumps. We propose a modification of the Hodrick-Prescott filter that contemplates jumps and automatically selects the time points in which the jumps occur. We provide an efficient implementation of the new filter in an R package. We use our modified filter to assess what Italian labour market reforms impacted employment in different age groups.

**Keywords:** Trend, State-space form, Unobserved component model, Structural change, LASSO, Business cycle, Employment

**JEL classification:** C22, C63, E32, J21

**Corresponding Author:**
Paolo Maranzano
Assistant Professor
Department of Economics, Management and Statistics, University of Milano-Bicocca
Via Bicocca degli Arcimboldi 8, Milan (Italy)
e-mail: paolo.maranzano@unimib.it

# Highlights

**A Hodrick-Prescott filter with automatically selected jumps**

Paolo Maranzano, Matteo Pelagatti

- We introduced a trend-cycle decomposition with jumps in the trend component
- An automatic procedure selects the time points of the jumps
- We implement our procedure efficiently in an R package
- The method identifies the significant impacts of reforms on employment in Italy

# A Hodrick-Prescott filter with automatically selected jumps

Paolo Maranzano[a,b], Matteo Pelagatti[a]

[a]*Department of Economics, Management and Statistics, University of Milano-Bicocca, Via Bicocca degli Arcimboldi, 8, Milano, 20126, MI, Italy*
[b]*Fondazione Eni Enrico Mattei, C.so Magenta, 63, Milano, 20123, MI, Italy*

**Abstract**

The Hodrick-Prescott filter is a popular tool in macroeconomics for decomposing a time series into a smooth trend and a business cycle component. The last few years have witnessed global events, such as the Global Financial Crisis, the COVID-19 pandemic, and the war in Ukraine, that have had abrupt structural impacts on many economic time series. Moreover, new regulations and policy changes generally lead to similar behaviours. Thus, those events should be absorbed by the trend component of the trend-cycle decomposition, but the Hodrick-Prescott filter does not allow for jumps. We propose a modification of the Hodrick-Prescott filter that contemplates jumps and automatically selects the time points in which the jumps occur. We provide an efficient implementation of the new filter in an R package. We use our modified filter to assess what Italian labour market reforms impacted employment in different age groups.

*Keywords:* Trend, State-space form, Unobserved component model, Structural change, LASSO, Business cycle, Employment
*JEL:* C22, C63, E32, J21

*Email addresses:* paolo.maranzano@unimib.it (Paolo Maranzano), matteo.pelagatti@unimib.it (Matteo Pelagatti)

## 1. Introduction

The Hodrick-Prescott (HP) filter (Hodrick and Prescott, 1981, 1997; Whittaker, 1922) is a very popular[1] tool in applied macroeconomics and related fields to split a time series into a low-frequency component, the trend, and a high-frequency component, the cycle (for a technical review refer to de Jong and Sakarya, 2016).

The HP filter solves a penalized least-square problem where a smoothness requirement balances the goodness of fit. A tuning parameter, whose value is generally set according to the sampling frequency of the time series (Ravn and Uhlig, 2002), determines the smoothness of the filter. Alternatively, its value can be estimated by Gaussian maximum likelihood (Gómez, 2001; Pelagatti, 2015, Sec. 3.2.3) exploiting the state-space form and the Kalman filter.

While the smoothness of the extracted trend is one of the main reasons for applying the HP filter, trends in time series can undergo abrupt changes because of exogenous interventions such as the recent pandemic, the war in Ukraine, or structural changes such as economic and social reforms. Of course, discontinuities in the trend component extracted by the HP filter can be achieved by splitting the time series into contiguous subsamples on which to apply separate HP filters. However, since it is not always possible to determine the precise dates of the jumps, it would be precious to have a filter that automatically detects the shifts in the trend component and adapts the extracted signal accordingly.

In the presence of jumps, the regular HP filter tends to smooth the abrupt changes out, introducing spurious cycles in its complement[2], which empirical macroeconomists use as an output-gap indicator. Indeed, a persistent change, such as a jump, belongs to the structural part of the economy and not to the business cycle. However, according to the standard HP filter, a persistent drop in the GDP would be classified as a short boom in the economy, followed by a temporary contraction of production, as Figure 1 illustrates. We simulated a time series by summing a linear trend with a drop from time

[1]The exact search "Hodrick Prescott filter" on Google Scholar returned 23,800 results on 6 June 2024.

[2]Here, we define the HP filter $\tau_t$ as the low-pass filter extracting the trend and, thus, its complement $y_t - \tau_t$ is the one used for business cycle analysis. Some scholars name the latter HP filter.

$t = 51$ with a stochastic cycle generated by an AR(2) process. We estimated the stochastic cycle realisation using the complement of the HP filter. The spurious cycle described above is evident in the shaded area in the figure: the actual positive phase of the cycle is substituted by a boost and a rapid recession.

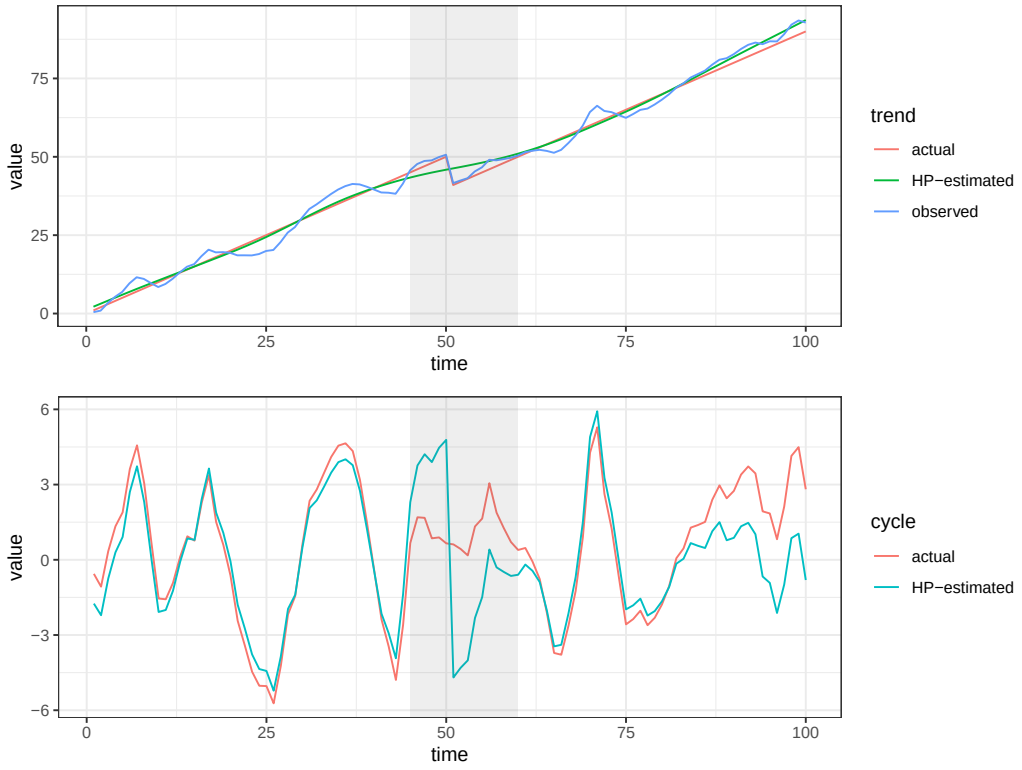


Figure 1: Extracting the trend and the output gap by HP filtering when a jump in the trend is present. The jump occurs at time $t = 51$.

In this paper, we propose a modification of the HP filter capable of automatically detecting structural changes by adding a potential jump at every time point and penalizing for the sum of their sizes. Well-known information criteria determine the magnitudes of the regularization parameters. Our method entails the constrained maximization of the Gaussian log-likelihood function with respect to a vast number of parameters, as there are more parameters than observations. However, our implementation in C++ and R (thanks to Rcpp by Eddelbuettel and François, 2011; Eddelbuettel, 2013)

is highly efficient, quick, and stable. Our approach exploits the state-space representation of the underlying data-generating process and allows missing observations and regressors, for example, for modelling seasonal patterns.

We assess our method's performance through a battery of simulation experiments, the outcomes of which are very encouraging.

Finally, a long section of the paper is devoted to analysing the impacts of various labour market reforms approved by the Italian Parliament on different generations of Italian workers. In particular, we apply our HP filter with jumps to the employment time series of the Italian population grouped by age to assess the different impacts that the reforms had on the age groups.

The structure of the paper is the following: Section 2 illustrates the method, Section 3 assesses the performance of the method on simulated time series, Section 4 applies the method to Italian employment time series, and Section 5 concludes.

## 2. Method

The HP filter is the sequence of linear functions $\tau_t = \sum_{s=1}^{n} \alpha_{t,s} y_s$ of the time series observations $\{y_t\}_{t=1,\dots,n}$ that solves

$$\min \left\{ \sum_{t=1}^{n} (y_t - \tau_t)^2 + \lambda \sum_{t=2}^{n-1} [(\tau_{t+1} - \tau_t) - (\tau_t - \tau_{t-1})]^2, \right\}$$

where $\lambda$ is a fixed parameter that determines the smoothness of the sequence $\{\tau_t\}_{t=1,\dots,n}$: the higher $\lambda$, the smoother the sequence. Indeed, the first addend in the objective function is a quadratic loss, while the second is a smoothness penalty. In other words, according to the first addend, the closer $\tau_t$ is to $y_t$, the better, while according to the second addend, the closer the second difference of $\tau_t$ to zero (i.e., the closer $\tau_t$ to a straight line), the better. When $\lambda$ diverges, $\tau_t$ becomes a linear trend. Typical values of $\lambda$ adopted in macroeconomic applications are 6.25 for yearly data, 1,600 for quarterly data, and 129,600 for monthly data; however, using the formulae in Ravn and Uhlig (2002), any sampling frequency can be mapped into a value of $\lambda$. These values of $\lambda$ produce a low-pass filter with a cut-off frequency corresponding to roughly ten years so that the time series is split into its trend and business cycle components[3].

[3]The value of $\lambda$ for which the gain of the filter is 0.5 is given by $(2\sin(\pi/p))^{-4}$, where $p$ is the cut-off period (cf. Gómez, 2001, p.366). For example, if we want the HP filter to extract

Gómez (2001) showed that the HP filter is the optimal linear predictor of the trend component $\mu_t$ based on the observations $\{y_t\}_{t=1,\dots,n}$ in the following unobserved component model:

$$\begin{aligned} y_t &= \mu_t + \varepsilon_t \\ \mu_{t+1} &= \mu_t + \beta_t + \eta_t \\ \beta_{t+1} &= \beta_t + \zeta_t, \end{aligned} \tag{1}$$

where $\varepsilon_t$, $\eta_t$, and $\zeta_t$ are independent white noise sequences with respective variances $\mathrm{Var}(\varepsilon_t) = \lambda\sigma^2$, $\mathrm{Var}(\eta_t) = 0$, and $\mathrm{Var}(\zeta_t) = \sigma^2$.

In equation (1), the time series $\mu_t$ represents the level of $y_t$, and $\beta_t$ is the time-varying slope of the trend. The sample paths of $\mu_t$ are smooth because the assumption $\mathrm{Var}(\eta_t) = 0$ prevents jumps. Indeed, the trend can only deviate from a straight line through slope changes.

Model (1) is in state-space form. The Kalman filter allows the (quasi) maximum likelihood estimation of the parameters $\sigma^2$ and $\lambda$ by assuming that the white noise sequences and the joint distribution of $(\mu_1, \beta_1)$ are Gaussian (see for example Pelagatti, 2015, Chapter 5). The smoother, say $\hat{\mu}_{t|n}$, which projects $\mu_t$ on the whole time series $\{y_t\}_{t=1,\dots,n}$, coincides with the HP filter: $\tau_t = \hat{\mu}_{t|n}$.

We introduce in the model (1) the possibility of abrupt changes in the level and slope by adding the variance sequence $\{\sigma_t^2\}_{t=1,\dots,n}$ to the constant variances of $\eta_t$ and $\zeta_t$ in the following way:

$$\mathrm{Var}(\eta_t) = \sigma_t^2, \qquad \mathrm{Var}(\zeta_t) = \sigma^2 + \gamma^2\sigma_t^2,$$

where $\gamma$ is a positive scaling parameter. The reasoning behind using just one sequence of additional variances common to the level and slope disturbances is based on the fact that, under structural changes, both components should be contemporaneously affected. Letting only the slope or the level change would be unusual in many real applications. At the same time, providing independent sequences of additional variances for the two transition equations would almost double the number of parameters to estimate and make change-points harder to identify. This choice does virtually no harm when only a

frequencies corresponding to a period of 10 years or longer in a yearly time series, we obtain $(2\sin(\pi/10))^{-4} \approx 6.85$, while if the data are quarterly, we get $(2\sin(\pi/40))^{-4} \approx 1,649$ and for monthly observations $(2\sin(\pi/120))^{-4} \approx 133,108$.

change in the level (or slope) takes place since the Kalman smoother adjusts to fit the observable time series even in the presence of a larger disturbance variance.

Under this time-varying variance configuration, the model (1) is no longer identified, but by penalizing the log-likelihood function by the sum of the additional standard deviations $\sigma_t$, we can get a simultaneous estimate of the parameters $\sigma^2$, $\lambda$, $\gamma$ and of the variances $\sigma_t^2$. The constrained optimization problem to solve is of LASSO type (see Hastie et al., 2009, Section 3.4.2)

$$\max_{\sigma,\lambda,\gamma,\{\sigma_t\}_{t=1,\dots,n}} \ell\big(\sigma,\lambda,\gamma,\{\sigma_t\}_{t=1,\dots,n}\big), \qquad \text{such that } \sum_{t=1}^{n}\sigma_t \le M, \tag{2}$$

where all parameters are positive, $\ell()$ is the Gaussian log-likelihood function (computed by the Kalman filter), and $M$ is a positive value to be fixed before the optimization. As we will discuss later, an effective way to determine the value of $M$ is by computing information criteria over a grid of values for $M$. The case $M = 0$ results in the classical HP filter, while $M \to \infty$ produces an unidentified model. The LASSO-type constraint in equation (2) implies that most supplementary variances $\sigma_t^2$ are set to zero, and only the ones that produce a significant improvement in the log-likelihood are allowed to have a positive value. Figure 3.11 of Hastie et al. (2009) contains a graphical explanation of this selection feature.

There are various algorithms that can solve this constrained optimization; in our simulations and applications, the *conservative convex separable approximations* (CCSA) method by Svanberg (2002), as implemented in the *NLopt* library (Johnson, 2007), has proven to be very quick, stable, and effective. Since the optimisation is carried out with respect to a very large vector of parameters, it is fundamental to provide the optimiser with analytical derivatives. We computed the relevant scores using the results in Koopman and Shephard (1992) (see Appendix A.6).

The degree of penalization in regularized models is usually determined by cross-validation (CV). However, in the typical application, time series are not very long, and jumps are rare; thus, CV would not work because the jumps would be excluded in many subsamples. A feasible approach is through information criteria. For every value of $M$ on a grid, we do the constrained optimization, evaluate the likelihood at the estimates, compute the degrees of freedom, and return the AIC, BIC, and HQ.

Since the smoother of $\mu_t$, say $\hat{\boldsymbol{\mu}} := \{\hat{\mu}_t\}_{t=1,\dots,n}$, is linear in the time series

vector $\boldsymbol{y} := \{y_t\}_{t=1,\dots,n}$, that it, there is a matrix $\boldsymbol{S}$ such that $\hat{\boldsymbol{\mu}} = \boldsymbol{S}\boldsymbol{y}$, then the number of *effective degrees of freedom* is given by the trace of the matrix $\boldsymbol{S}$ (see Hastie et al., 2009, Chapter 5). The elements of the matrix $\boldsymbol{S}$ (we are interested only in its diagonal) can be easily computed by adapting the formulae in Koopman and Harvey (2003).

For illustration, we applied the HP filter with jumps to a simulated time series and to the famous Nile River time series[4]. The simulated time series is generated by adding zero-mean Gaussian noise (with a standard deviation of 20) to the following signal function of $t = 1, 2, \dots, 100$:

$$100\cos(3t\pi/100) - 100\,\mathbb{I}_{(t>50)} - 10\,(t-50)\,\mathbb{I}_{(t>50)},$$

with $\mathbb{I}_{(t>50)}$ equal to zero when $t <= 50$ and to one for $t > 50$.

The top panel of Figure 2 illustrates how the HP filter with jumps captures the jump taking place between the $50^{\text{th}}$ and $51^{\text{st}}$ observations and how precise is the estimate of the mean function. The bottom panel of the same figure shows how the well-known jump in the year 1899 (Cobb, 1978; Carlstein, 1988; Dümbgen, 1991) is perfectly captured by our filter, and the trend of the time series turns out to be piecewise constant as the estimated smoothing parameter is extremely large. A sound economic application is discussed in Section 4.

The observation equation of the state-space form in equation (1) can be easily modified to include linear regressors in the model: $y_t = \boldsymbol{x}_t^\top \boldsymbol{\delta} + \mu_t + \varepsilon_t$, where $\boldsymbol{x}_t$ is the vector of regressors and $\boldsymbol{\delta}$ a vector of coefficients to be estimated. This setup is particularly useful for adding seasonal patterns that, otherwise, the HP filter (with and without jumps) would try to fit. To avoid changing the interpretation of the HP filter as a trend extractor, the regression part $\boldsymbol{x}_t^\top \boldsymbol{\delta}$ should sum to zero over an opportune period of time (as seasonal sinusoids and centred seasonal dummies).

## 3. Simulations

Our HP filter with jumps is designed to deal with macroeconomic time series whose typical length is rarely longer than 100 observations and which are affected by a small number of jumps. As only $\lambda$, the ratio between the

[4]The time series represents the volume of the Nile River at Aswan for the years 1871 to 1970.

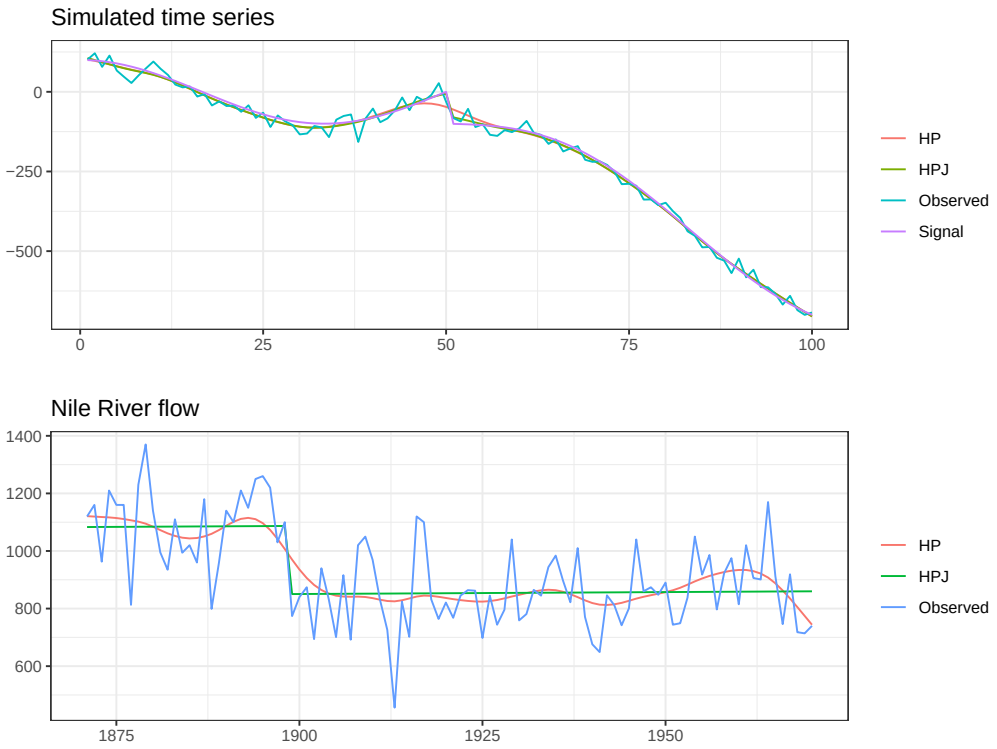


Figure 2: HP filter with and without jumps applied to (top) the artificial time series and (bottom) the Nile volume time series.

variances of $\varepsilon_t$ and $\zeta_t$, is relevant for the filter, in the simulations, we set $\sigma = 1$ and change $\lambda$.

The data-generating process is equation (1), and the simulation design is summarised in the following lines.

**Jump number** The number of jumps is 1, 2, and 3. No jumps occur in the first and last four time points of the simulated time series.

**Noise-to-signal ratio** The standard deviation of the slope disturbance $\zeta_t$ is set to 1, while the standard deviation of the observation noise gets the values $\{20, 40, 80\}$ that imply a noise-to-signal ratio $\lambda$ equal to $\{400, 1600, 6400\}$.

**Jump sizes** The jumps occur simultaneously in the level and in the slope, and their sizes are $\{5, 10, 15\}$ times $\sqrt{\lambda}\sigma$ for the level and $\sigma$ for the

slope.

**$M$-grid** For every aforementioned configuration, the grid of $M$ values on which the optimization is carried out is $\{0, 10, 20, \ldots, 1000\}$.

Our filtering procedure is evaluated both as a signal extraction method and as a change-point estimator. The first objective is accomplished by computing the mean square error (MSE) of the extracted signal with respect to the real signal generated in each simulation. The second objective is summarized by the true positive rate (TPR) and true negative rate (TNR) and their semisum, which is generally referred to as *balanced accuracy*. Guessing by the most probable class (in this case, not being a change-point) implies a balanced accuracy of 0.5 (the TPR equals zero and the TNR equals one).

For every combination of the number of jumps, jump size, and noise-to-signal ratio, Table 1 reports the relative efficiency of our filter compared to the HP filter, that is, the ratio of the MSE of the signal extracted by the HP filter with regularization parameter $M$ selected according to various information criteria to the MSE of the standard HP filter. Therefore, values larger than 1 imply that the variability of HP filter with jumps is lower compared to that of the standard HP filter. The last column displays the same ratio for the best *ex-post* choice of $M$ on the grid. The fourth column indicates the information criterion that archives the minimum MSE among the four ICs considered.

According to Table 1, when jumps are present, the MSE of the filter with jumps always performs better than the classical HP filter, with the best gain in terms of MSE for larger numbers of jumps, larger jump sizes, and larger noise-to-signal ratios. The best information criterion for selecting the value of $M$ is, on average, BIC, but HQ comes very close.

The unexpected result is that even when there are no jumps, for high noise-to-signal processes, the introduction of jumps can be beneficial (cf. the BIC and BEST MSE columns).

The best results for the true positive rate (TPR) are obtained using the AIC (cf. Table 2). This fact is not surprising, as the AIC selects the largest number of jumps among the information criteria, increasing the probability of selecting the actual jumps. However, the TPRs of the other information criteria are close to AIC's. On the contrary, as evident from Table 3, the BIC is the information criterion that achieves the largest true negative rate (TNR). This was also expected, being BIC the criterion that selects the

Table 1: Relative efficiency of the HP with jumps with respect to the standard HP.

| JUMPS | | | INFO CRITERIA | | | | | BEST |
|---|---|---|---|---|---|---|---|---|
| N. | SIZES | $\lambda$ | BEST | AIC | AICC | BIC | HQ | MSE |
| 0 | - | 400 | BIC | 0.4 | 0.5 | 0.7 | 0.5 | 1.0 |
| 0 | - | 1600 | BIC | 0.5 | 0.6 | 0.9 | 0.7 | 1.1 |
| 0 | - | 6400 | BIC | 0.7 | 0.8 | 1.2 | 0.9 | 1.4 |
| 1 | 5 | 400 | BIC | 1.2 | 1.4 | 1.9 | 1.5 | 2.4 |
| 1 | 5 | 1600 | BIC | 1.6 | 1.8 | 2.3 | 1.9 | 3.1 |
| 1 | 5 | 6400 | BIC | 2.1 | 2.2 | 2.7 | 2.3 | 3.7 |
| 1 | 10 | 400 | BIC | 4.5 | 4.9 | 6.1 | 5.2 | 8.2 |
| 1 | 10 | 1600 | BIC | 5.5 | 6.0 | 7.6 | 6.3 | 10.4 |
| 1 | 10 | 6400 | BIC | 7.5 | 7.7 | 9.2 | 8.0 | 12.1 |
| 1 | 15 | 400 | BIC | 10.3 | 11.4 | 13.4 | 11.7 | 17.8 |
| 1 | 15 | 1600 | BIC | 12.6 | 13.7 | 16.5 | 14.3 | 22.2 |
| 1 | 15 | 6400 | BIC | 17.6 | 17.6 | 19.6 | 18.8 | 25.4 |
| 2 | 5 | 400 | BIC | 1.9 | 2.2 | 2.6 | 2.3 | 3.6 |
| 2 | 5 | 1600 | BIC | 2.3 | 2.6 | 2.8 | 2.7 | 4.1 |
| 2 | 5 | 6400 | HQ | 2.8 | 3.0 | 2.9 | 3.0 | 4.3 |
| 2 | 10 | 400 | BIC | 7.4 | 8.3 | 10.0 | 8.5 | 13.6 |
| 2 | 10 | 1600 | BIC | 8.9 | 9.6 | 10.9 | 9.9 | 15.8 |
| 2 | 10 | 6400 | HQ | 12.2 | 12.0 | 11.2 | 12.4 | 16.0 |
| 2 | 15 | 400 | BIC | 16.2 | 18.3 | 21.4 | 18.6 | 29.8 |
| 2 | 15 | 1600 | BIC | 21.2 | 22.2 | 25.6 | 22.7 | 33.7 |
| 2 | 15 | 6400 | HQ | 29.4 | 30.0 | 30.4 | 30.4 | 35.8 |
| 3 | 5 | 400 | BIC | 2.4 | 2.8 | 3.0 | 2.8 | 4.3 |
| 3 | 5 | 1600 | HQ | 2.9 | 3.2 | 3.2 | 3.3 | 4.9 |
| 3 | 5 | 6400 | AICC | 3.6 | 3.6 | 3.1 | 3.6 | 4.9 |
| 3 | 10 | 400 | BIC | 9.3 | 10.9 | 12.5 | 10.9 | 17.2 |
| 3 | 10 | 1600 | BIC | 12.3 | 12.6 | 13.3 | 13.0 | 19.4 |
| 3 | 10 | 6400 | HQ | 16.9 | 16.8 | 14.3 | 17.2 | 19.3 |
| 3 | 15 | 400 | BIC | 22.0 | 25.2 | 28.6 | 24.9 | 39.6 |
| 3 | 15 | 1600 | BIC | 32.4 | 33.1 | 35.4 | 33.6 | 44.5 |
| 3 | 15 | 6400 | BIC | 37.1 | 36.7 | 39.2 | 38.7 | 43.8 |

Table 2: True positive rate (%) of our method detecting actual jumps.

| JUMPS | | | INFO CRITERIA | | | | | BEST |
|---|---|---|---|---|---|---|---|---|
| N. | SIZES | $\lambda$ | BEST | AIC | AICC | BIC | HQ | MSE |
| 1 | 5 | 20 | AIC | 95.2 | 94.8 | 94.0 | 94.4 | 95.8 |
| 1 | 5 | 40 | AIC | 88.8 | 88.6 | 87.2 | 88.3 | 90.1 |
| 1 | 5 | 80 | AIC | 87.6 | 87.3 | 83.2 | 86.8 | 88.8 |
| 1 | 10 | 20 | AIC | 99.8 | 99.8 | 99.8 | 99.8 | 100.0 |
| 1 | 10 | 40 | AIC | 99.8 | 99.8 | 99.7 | 99.8 | 99.9 |
| 1 | 10 | 80 | AIC | 99.8 | 99.8 | 98.5 | 99.5 | 100.0 |
| 1 | 15 | 20 | AIC | 100.0 | 100.0 | 99.9 | 100.0 | 99.8 |
| 1 | 15 | 40 | AIC | 100.0 | 100.0 | 99.8 | 100.0 | 100.0 |
| 1 | 15 | 80 | AIC | 100.0 | 100.0 | 99.0 | 100.0 | 100.0 |
| | | | | | | | | |
| 2 | 5 | 20 | AIC | 94.8 | 94.2 | 91.3 | 93.8 | 95.2 |
| 2 | 5 | 40 | AIC | 89.2 | 89.0 | 84.0 | 88.5 | 91.0 |
| 2 | 5 | 80 | AIC | 85.2 | 84.4 | 77.9 | 83.9 | 86.7 |
| 2 | 10 | 20 | AIC | 99.9 | 99.7 | 99.4 | 99.7 | 99.6 |
| 2 | 10 | 40 | AIC | 99.8 | 99.6 | 97.8 | 99.5 | 99.6 |
| 2 | 10 | 80 | AIC | 99.3 | 98.8 | 93.5 | 98.5 | 99.9 |
| 2 | 15 | 20 | AIC | 99.9 | 99.9 | 99.8 | 99.9 | 99.9 |
| 2 | 15 | 40 | AIC | 99.9 | 99.8 | 99.5 | 99.8 | 99.9 |
| 2 | 15 | 80 | AIC | 100.0 | 99.9 | 99.2 | 99.9 | 100.0 |
| | | | | | | | | |
| 3 | 5 | 20 | AIC | 93.4 | 93.0 | 89.1 | 92.5 | 94.8 |
| 3 | 5 | 40 | AIC | 89.4 | 89.1 | 83.3 | 88.6 | 91.9 |
| 3 | 5 | 80 | AIC | 86.2 | 84.8 | 76.4 | 84.1 | 88.5 |
| 3 | 10 | 20 | AIC | 99.8 | 99.7 | 99.1 | 99.7 | 99.8 |
| 3 | 10 | 40 | AIC | 99.5 | 99.4 | 97.7 | 99.4 | 99.8 |
| 3 | 10 | 80 | AIC | 99.6 | 99.3 | 95.7 | 99.2 | 99.9 |
| 3 | 15 | 20 | AIC | 100.0 | 99.9 | 99.9 | 99.9 | 99.9 |
| 3 | 15 | 40 | AIC | 99.9 | 99.9 | 99.6 | 99.9 | 99.8 |
| 3 | 15 | 80 | AIC | 100.0 | 99.8 | 99.5 | 99.8 | 100.0 |

Table 3: True negative rate (%) of our method detecting actual jumps.

| JUMPS | | | INFO CRITERIA | | | | | BEST |
|---|---|---|---|---|---|---|---|---|
| N. | SIZES | $\lambda$ | BEST | AIC | AICC | BIC | HQ | MSE |
| 0 | 0 | 20 | BIC | 91.6 | 93.7 | 96.5 | 94.2 | 99.8 |
| 0 | 0 | 40 | BIC | 94.0 | 95.2 | 97.6 | 95.8 | 99.1 |
| 0 | 0 | 80 | BIC | 95.8 | 96.3 | 98.2 | 97.0 | 98.6 |
| 1 | 5 | 20 | BIC | 91.9 | 93.4 | 97.2 | 94.4 | 98.3 |
| 1 | 5 | 40 | BIC | 93.8 | 94.9 | 97.5 | 95.6 | 98.6 |
| 1 | 5 | 80 | BIC | 95.7 | 96.3 | 97.9 | 96.6 | 98.5 |
| 1 | 10 | 20 | BIC | 93.8 | 94.6 | 97.0 | 95.4 | 98.6 |
| 1 | 10 | 40 | BIC | 95.0 | 95.8 | 97.6 | 96.2 | 98.6 |
| 1 | 10 | 80 | BIC | 96.4 | 96.5 | 97.9 | 96.9 | 97.9 |
| 1 | 15 | 20 | BIC | 94.5 | 95.5 | 97.2 | 95.9 | 98.7 |
| 1 | 15 | 40 | BIC | 95.2 | 96.1 | 97.9 | 96.6 | 98.7 |
| 1 | 15 | 80 | BIC | 96.9 | 96.6 | 97.9 | 97.1 | 97.9 |
| 2 | 5 | 20 | BIC | 91.4 | 93.9 | 97.0 | 94.4 | 98.4 |
| 2 | 5 | 40 | BIC | 93.1 | 94.8 | 97.3 | 95.3 | 98.1 |
| 2 | 5 | 80 | BIC | 95.1 | 95.6 | 97.4 | 95.8 | 95.4 |
| 2 | 10 | 20 | BIC | 92.3 | 94.1 | 96.5 | 94.6 | 98.3 |
| 2 | 10 | 40 | BIC | 93.7 | 94.6 | 97.1 | 94.8 | 97.7 |
| 2 | 10 | 80 | BIC | 95.6 | 95.4 | 96.5 | 96.0 | 93.5 |
| 2 | 15 | 20 | BIC | 92.7 | 94.4 | 96.4 | 94.8 | 98.3 |
| 2 | 15 | 40 | BIC | 94.7 | 95.0 | 96.8 | 95.5 | 97.6 |
| 2 | 15 | 80 | BIC | 95.6 | 95.8 | 96.5 | 95.9 | 95.4 |
| 3 | 5 | 20 | BIC | 90.7 | 93.5 | 96.4 | 93.9 | 97.8 |
| 3 | 5 | 40 | BIC | 92.6 | 93.8 | 96.8 | 94.6 | 97.1 |
| 3 | 5 | 80 | BIC | 95.1 | 95.4 | 96.1 | 95.8 | 91.6 |
| 3 | 10 | 20 | BIC | 90.6 | 93.4 | 95.9 | 93.6 | 97.7 |
| 3 | 10 | 40 | BIC | 93.5 | 93.7 | 96.0 | 94.3 | 96.9 |
| 3 | 10 | 80 | BIC | 94.2 | 94.3 | 95.6 | 94.7 | 90.5 |
| 3 | 15 | 20 | BIC | 91.7 | 93.9 | 95.7 | 93.8 | 97.8 |
| 3 | 15 | 40 | BIC | 95.1 | 95.3 | 96.4 | 95.5 | 97.0 |
| 3 | 15 | 80 | BIC | 94.7 | 94.5 | 95.6 | 95.2 | 94.8 |

Table 4: Balanced accuracy (%) of our method detecting actual jumps.

| JUMPS | | | INFO CRITERIA | | | | | BEST |
|---|---|---|---|---|---|---|---|---|
| N. | SIZES | $\lambda$ | BEST | AIC | AICC | BIC | HQ | MSE |
| 1 | 5 | 20 | BIC | 93.6 | 94.1 | 95.6 | 94.4 | 97.0 |
| 1 | 5 | 40 | BIC | 91.3 | 91.7 | 92.3 | 91.9 | 94.3 |
| 1 | 5 | 80 | AICC | 91.6 | 91.8 | 90.5 | 91.7 | 93.6 |
| 1 | 10 | 20 | BIC | 96.8 | 97.2 | 98.4 | 97.6 | 99.3 |
| 1 | 10 | 40 | BIC | 97.4 | 97.8 | 98.6 | 98.0 | 99.3 |
| 1 | 10 | 80 | BIC | 98.1 | 98.1 | 98.2 | 98.2 | 98.9 |
| 1 | 15 | 20 | BIC | 97.2 | 97.8 | 98.5 | 98.0 | 99.3 |
| 1 | 15 | 40 | BIC | 97.6 | 98.1 | 98.8 | 98.3 | 99.4 |
| 1 | 15 | 80 | HQ | 98.4 | 98.3 | 98.4 | 98.6 | 99.0 |
| 2 | 5 | 20 | BIC | 93.1 | 94.0 | 94.1 | 94.1 | 96.8 |
| 2 | 5 | 40 | AICC | 91.1 | 91.9 | 90.6 | 91.9 | 94.5 |
| 2 | 5 | 80 | AIC | 90.2 | 90.0 | 87.6 | 89.8 | 91.0 |
| 2 | 10 | 20 | BIC | 96.1 | 96.9 | 98.0 | 97.1 | 98.9 |
| 2 | 10 | 40 | BIC | 96.8 | 97.1 | 97.4 | 97.1 | 98.6 |
| 2 | 10 | 80 | AIC | 97.5 | 97.1 | 95.0 | 97.2 | 96.7 |
| 2 | 15 | 20 | BIC | 96.3 | 97.1 | 98.1 | 97.3 | 99.1 |
| 2 | 15 | 40 | BIC | 97.3 | 97.4 | 98.1 | 97.6 | 98.7 |
| 2 | 15 | 80 | HQ | 97.8 | 97.8 | 97.8 | 97.9 | 97.7 |
| 3 | 5 | 20 | AICC | 92.0 | 93.2 | 92.8 | 93.2 | 96.3 |
| 3 | 5 | 40 | HQ | 91.0 | 91.4 | 90.1 | 91.6 | 94.5 |
| 3 | 5 | 80 | AIC | 90.6 | 90.1 | 86.2 | 89.9 | 90.0 |
| 3 | 10 | 20 | BIC | 95.2 | 96.6 | 97.5 | 96.6 | 98.7 |
| 3 | 10 | 40 | HQ | 96.5 | 96.5 | 96.9 | 96.9 | 98.4 |
| 3 | 10 | 80 | HQ | 96.9 | 96.8 | 95.6 | 97.0 | 95.2 |
| 3 | 15 | 20 | BIC | 95.9 | 96.9 | 97.8 | 96.9 | 98.8 |
| 3 | 15 | 40 | BIC | 97.5 | 97.6 | 98.0 | 97.7 | 98.4 |
| 3 | 15 | 80 | BIC | 97.4 | 97.1 | 97.5 | 97.5 | 97.4 |

smallest number of jumps. The TNR increases with noise-to-signal ratio and jump size.

Table 4 summarises the two rates in the Balanced Accuracy (BA) value, defined as the semisum of TPR and TNR. If one classifies each observation by the most probable value, that is, "not a jump", then the BA is equal to 0.5 (the semisum of a TPR of 0 and a TNR of 1). All the numbers we obtained are well above 0.5, with BIC selecting the best result most of the time and being very close to the best result even when it does not provide the best choice. We stress that the HP filter with jump presented here performs a smooth signal extraction in the presence of discontinuities, thus it is not a purely tool for changepoints detections. However, the simulation results suggest a good balance between size and power (i.e., the TPR is high, and its complement to 1 is close to the classical 1% or 5% levels).

## 4. Assessing structural breaks in the Italian labor market

The last few years have witnessed global events, such as the Global Financial Crisis and the Great Recession (2008-2011), the COVID-19 pandemic in 2020-2021, and the war in Ukraine (2022-on), that have had abrupt structural impacts on many socio-economic economic indicators (Fazzari and Needler, 2021; Shibata, 2021). European countries adopted a vast portfolio of structural reforms in several fields of interventions. As remarked by Tito (2011), among the EU-28 countries, the large majority increased its activism by intensifying the interventions in labour market policy programmes or by adjusting taxes and benefits for low-wage earners. An intense increase in the degree of European reformism has thus led to large variations in the effectiveness across the EU member states (D'Auria et al., 2009). For instance, countries with a lower propensity to invest in new technologies and research would benefit the most from promoting and skill-upgrading policies; also, output and employment benefit from the introduction of political measures improving the composition of the labour force toward more skilled profiles or increasing the financial integrations and removing entry barriers in certain markets, such as the final good market (Roeger and Varga, 2008).

Among the Western countries, Italy was one of the most deeply involved in implementing structural reforms that impacted the whole economy, particularly the national labour markets and fostered socio-economic changes. Between 2011 and 2017, some of the most relevant reforms concerned the liberalization of services, incentives for business innovation, and a new structure

of the civil justice system to improve court efficiency (Ciapanna et al., 2020). The labour market has received considerable national and supranational political attention, resulting in more than twenty legislative interventions since the Nineties. Some of the interventions were minor adjustments, while others had significant relevance, such as the fixed-term contracts reform in 2001 (Legislative Decree no. 368/2001) or the reform of apprenticeship contracts in 2003 (the so-called "Biagi Law") (Gnocato et al., 2020) or the *Jobs Act* of 2015 that revised the rules governing layoffs and introduced a new contract with increasing protections (Nannicini et al., 2019). According to (Cappellari et al., 2012), the 2001 reform of fixed-term contracts induced a substitution of temporary employees in favour of external staff and reduced capital intensity, generating productivity losses; conversely, the Biagi reform of apprenticeship contracts increased job turnover and induced the substitution of external staff with firms' apprentices, with an overall productivity-enhancing effect. The effects of the *Jobs Act* reform are still uncertain. For instance, Berton et al. (2023) estimate that the impact of incentives on generating permanent contracts is higher in regions with a robust socio-economic and institutional ground, while the reduced firing costs did not generate significant direct impacts, with negligible cross-regional patterns, whereas Fana et al. (2016) show that the expected boost in employment was missing and that both the share of temporary contracts and the number of part-time contracts increased. The welfare and social security system has also undergone major changes, starting with the Monti-Fornero Pension Reform of 2012, which significantly postponed the retirement ages and almost cancelled the so-called seniority pensions (Fornero, 2014). Such reform decreased the level of labour protection only for medium and large firms above the 15-employee cut-off while weakly increasing the number of trained workers in firms due to the reduction in worker turnover and higher use of permanent contracts (Bratti et al., 2021).

Such an intricate and puzzling situation leads us to conjecture that the combination of structural reforms and socio-economic shocks has generated structural changes in the number of people employed within the country. Additionally, we assume that pensions and contract reforms had heterogeneous effects across age classes. In particular, while pension reforms mainly influenced the senior workers market, the contracts and apprenticeship reforms impacted younger workers. Other macroeconomic events had a relevant impact on the Italian labour market.

To test the previous research hypothesis, we employ the HP filter with

jumps to identify structural breaks in the quarterly time series of employed workers in Italy for different age groups from 1993 to 2023 (1993Q1-2023Q4). In particular, we considered the following age classes: 15 to 24 years old; 15 to 29 years old; 25 to 29 years old; 25 to 54 years old; 29 to 54 years old; 55 to 64 years old; 15 to 64 years old. Data were collected from the Eurostat (2024) *Employment and activity by sex and age* database.

Following OECD (2023, 2024) definition, we refer to people between 15 and 24 years as workers entering the labour market following education (hereafter, junior workers), people from 25 to 54 years as workers in their prime working lives (hereafter, intermediate workers), and people from 55 to 64 years as workers passing the peak of their career and approaching retirement (hereafter, senior workers). Altogether, workers aged 15 to 64 constitute the overall Italian working-age population. In the following, we only discuss results for the above-mentioned four age classes for brevity. However, due to the considerable importance of the 25- to 54-year-old age group in the Italian labour market (out of about 23 million workers, about 17 fall into this class), we also discuss an in-depth breakdown of this group by dividing it into two segments: early-career employed (25-29 years) and experienced employed (29-54 years). Eurostat data on these segments cover only 2009 to 2023 (2009Q1-2023Q4). Regarding the other non-mentioned age classes, workers from 15 to 74 years old, from 20 to 64 years old, and from 29 to 74 years old, we refer the reader to the Supplementary Materials containing extended empirical results.

In Figure 3, we show the actual, HP-filtered and HPJ-filtered time series for the junior (top left), intermediate (top right), and senior employed persons (bottom left), as well as for the overall working age population (bottom right). The vertical lines represent the structural breaks identified by the HP with jumps using the BIC criterion.

Looking at Figure 3, we can draw the following considerations. Junior and senior workers follow inverse trajectories and are affected by different shocks. Indeed, with the population ageing process and the gradual retirement age rise, the employment of seniors is increasing. The negative trend of juniors is consistent with the low Italian birth rate and the increase in the young population remaining in education and entering the labour market later. Also, junior workers experience sudden changes that quickly reabsorb, while seniors are driven by slow but radical changes. Furthermore, junior and

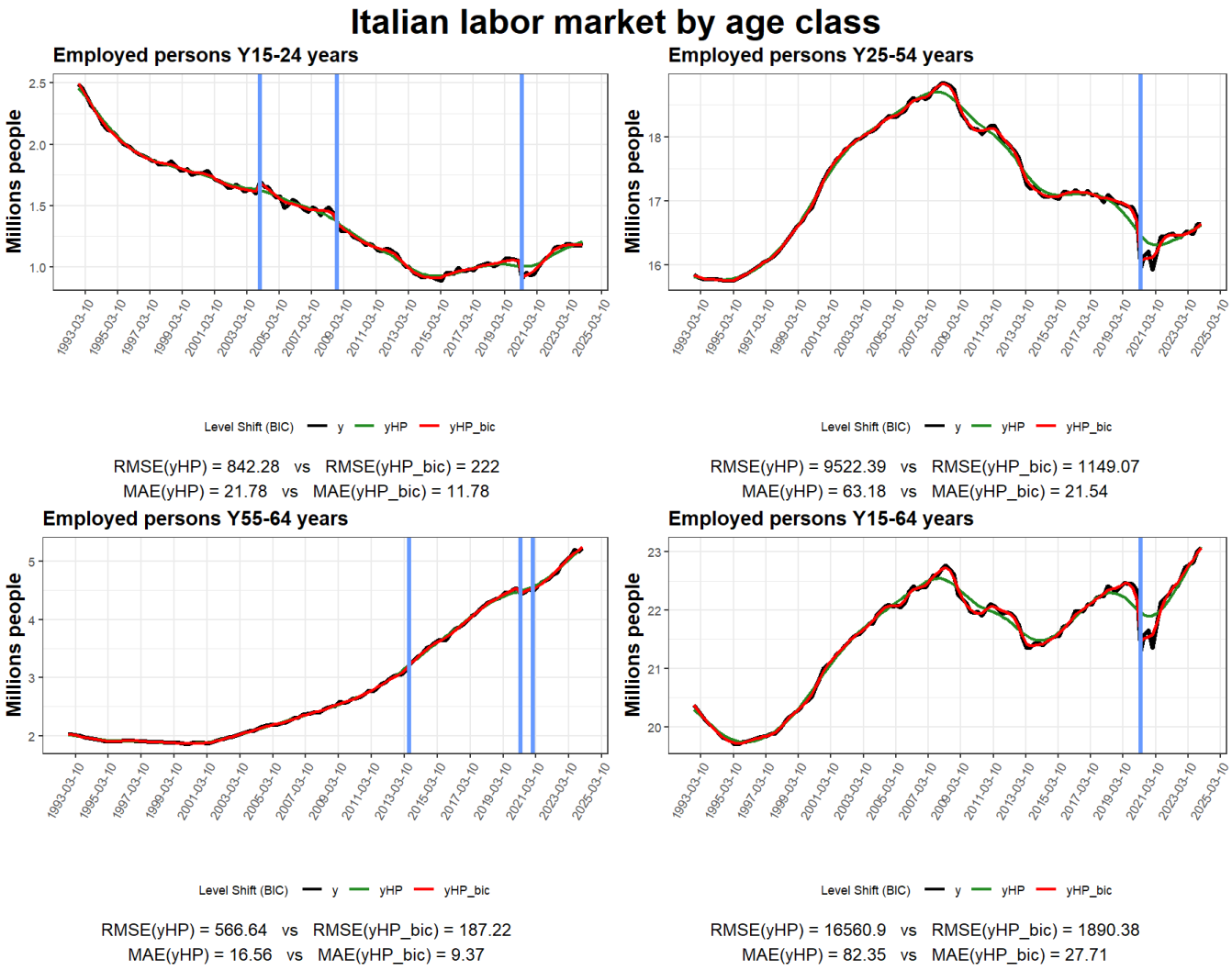


Figure 3: Actual and smoothed time series for employed persons in Italy by age class. Black curves represent the raw data; the vertical lines represent the structural breaks identified by the HPJ using the BIC; Green curves (yHP) are the smoothed values using the basic HP filter; red curves (yHP_bic) are the smoothed values produced by the HP filter with jumps. Under each subplot, we report the two smoothers' root mean squared error (RMSE) and mean absolute error (MAE).

intermediate workers seem to follow the business cycle (pro-cyclical) with sudden changes quickly reabsorbed, while seniors are driven by slow but radical (almost linear) changes. The HP filter with jumps identifies four of the political and macroeconomic events discussed above.

1. *The Biagi reform of apprenticeship contracts in 2003.* The series of junior workers had a clear positive jump at the beginning of that year, but this was immediately absorbed by the end of the year.
2. *The Great Recession of 2008-2009.* The junior worker series suffered a noticeable negative jump in the fourth quarter of 2008 when employment declined by several thousand. Conversely, the HPJ filter does not identify a shock for the working-age population or the intermediate workers despite the noticeable change in slopes (positive to negative). For the senior market, the series shows no jumps or changes in slope.
3. *The implementation of the Monti-Fornero Reform between 2012 and 2013.* The filter identifies a structural break (probably a change in slope) in the months following the enforcement of the pension and retirement age reform only for the senior worker series.
4. *COVID-19 pandemic in 2020-2021.* For all ages, the pandemic is the structural break that generated the greatest consequences. In fact, while 2020 shows the largest reductions in the number of employed people among the various events considered, in 2021, employment increases rapidly, surpassing pre-pandemic values.

In Figure 4, we show the actual and smoothed time series for the early-career (left) and experienced (right) workers.

The split into the two sub-classes clearly shows the differential effects of socio-economic and political events on workers who have recently entered the market and those in their careers. While for experienced workers, only the negative role of the COVID-19 pandemic is confirmed, for early-career jobs, the findings are more complex. In fact, the initial downward dynamics consistent with the aftermath of the Great Recession decelerated in 2010-2013 and accelerated in 2012-2014 with a sharp turnaround in 2014. Between 2014 and 2015, the *Jobs Act* was enacted, introducing contracts with gradually increasing protections for young new hires and tax breaks for firms that hired through permanent contracts. However, it is worth mentioning that the same period represents a time of general growth for the country and for the entire European Union.

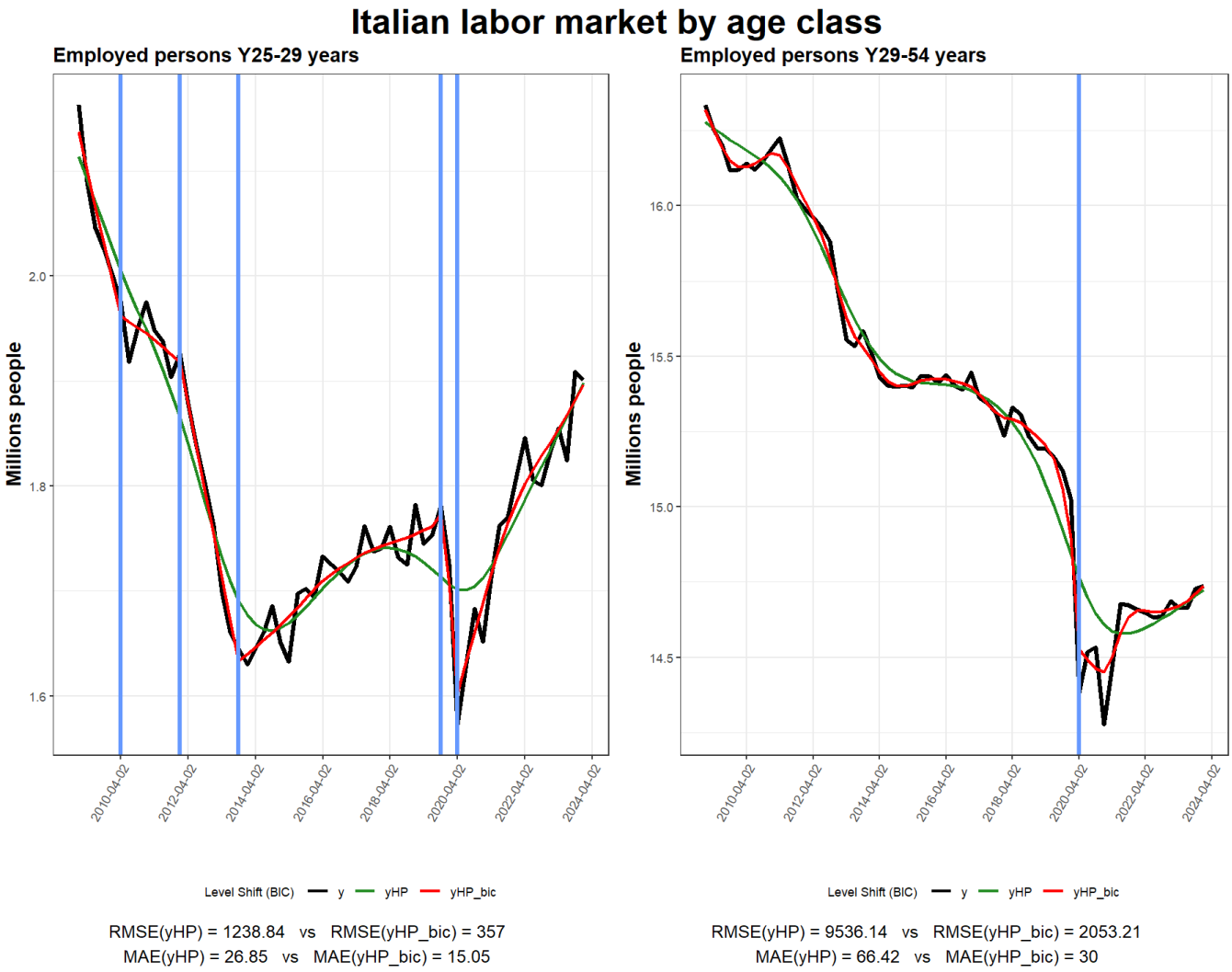


Figure 4: Actual and smoothed time series series for employed persons in Italy by age class. Black curves represent the raw data; vertical lines represent the structural breaks identified by the HPJ using the BIC; green curves (yHP) are the smoothed values using the basic HP filter; red curves (yHP_bic) are the smoothed values produced by the HP jumps filter. Under each subplot, we report the two smoothres' root mean squared error (RMSE) and mean absolute error (MAE).

## 5. Conclusions

We introduced a modification of the ubiquitous Hodrick-Prescott filter that allows for automatically detected jumps. The identification and estimation of the jumps exploit the state-space representation of the model underlying the HP filter. We let the smooth component have a possible jump in level and slope at every single time point and regularise the log-likelihood of the model so that the size of each jump must bring a significant increase in the log-likelihood to break away from zero. The optimal number and size of jumps are controlled through information criteria, and BIC performs the best.

Our method can be seen as a signal extraction procedure for a smooth signal with few discontinuities rather than as a test for changepoints. However, the simulation experiments and applications discussed in this paper show that our procedure also works well when evaluated as a changepoint test by reaching a good balance between size and power.

We implemented the procedure in the R package *jumps*, which allows the application of the HP filter with automatically selected jumps by selecting the amount of regularization on a grid of $M$ values (cf. Equation 2). The user can provide the value of the smoothing constant $\lambda$ or estimate its value by maximum likelihood. Regressors such as centred seasonal dummies or sinusoids can and should be added to the model (1) if present in the data. Our R package implements this extension experimentally. We did extensive work to ensure that the software was implemented in the fastest and most stable way. The interested reader can find all the formulae for implementing an efficient HP filter with jumps in any computer language in the appendix.

## References

Berton, F., Pacelli, L., Quaranta, R., Trentini, F., 2023. Patterns of labor market reforms: a regional approach to the Italian 'Jobs Act'. Inapp.

Bratti, M., Conti, M., Sulis, G., 2021. Employment protection and firm-provided training in dual labour markets. Labour Economics 69, 101972. doi:10.1016/j.labeco.2021.101972.

Cappellari, L., Dell'Aringa, C., Leonardi, M., 2012. Temporary employment, job flows and productivity: A tale of two reforms. The Economic Journal 122, F188–F215. doi:10.1111/j.1468-0297.2012.02535.x.

Carlstein, E., 1988. Nonparametric change-point estimation. The Annals of Statistics 16, 188–197. doi:10.1214/aos/1176350699.

Ciapanna, E., Mocetti, S., Notarpietro, A., 2020. The effects of structural reforms. evidence from italy. Report Banca d'Italia .

Cobb, G.W., 1978. The problem of the Nile: Conditional solution to a changepoint problem. Biometrika 65, 243–251. doi:10.1093/biomet/65.2.243.

D'Auria, F., Pagano, A., Ratto, M., Varga, J., 2009. A comparison of structural reform scenarios across the EU member states: Simulation-based analysis using the QUEST model with endogenous growth. Technical Report. Directorate General Economic and Financial Affairs (DG ECFIN), European Commission.

Dümbgen, L., 1991. The asymptotic behavior of some nonparametric change-point estimators. The Annals of Statistics 19, 1471–1495. doi:10.1214/aos/1176348257.

Eddelbuettel, D., 2013. Seamless R and C++ Integration with Rcpp. Springer, New York. doi:10.1007/978-1-4614-6868-4.

Eddelbuettel, D., François, R., 2011. Rcpp: Seamless R and C++ integration. Journal of Statistical Software 40, 1–18. doi:10.18637/jss.v040.i08.

Eurostat, 2024. Employment and activity by sex and age - quarterly data (1989-2024). doi:0.2908/LFSI_EMP_Q.

Fana, M., Guarascio, D., Cirillo, V., 2016. Did italy need more labour flexibility? Intereconomics 51, 79–86. doi:10.1007/s10272-016-0581-3.

Fazzari, S.M., Needler, E., 2021. Us employment inequality in the great recession and the covid-19 pandemic. European Journal of Economics and Economic Policies 18, 223–239.

Fornero, E., 2014. Economic-financial literacy and (sustainable) pension reforms: why the former is a key ingredient for the latter. Netspar Discussion Paper No. 02/2014-098 doi:http://dx.doi.org/10.2139/ssrn.2665089.

Gnocato, N., Modena, F., Tomasi, C., 2020. Labor market reforms and allocative efficiency in italy. Labour Economics 67, 101938. doi:https://doi.org/10.1016/j.labeco.2020.101938.

Gómez, V., 2001. The use of Butterworth filters for trend and cycle estimation in economic time series. Journal of Business & Economic Statistics 19, 365–373. doi:10.1198/073500101681019909.

Hastie, T., Tibshirani, R., Friedman, J., 2009. The Elements of Statistical Learning. Data Mining, Inference, and Prediction. Second ed., Springer.

Hodrick, R.J., Prescott, E.C., 1981. Postwar U.S. Business Cycles: An Empirical Investigation. Discussion Paper 451. Northwestern University, Kellogg School of Management, Center for Mathematical Studies in Economics and Management Science.

Hodrick, R.J., Prescott, E.C., 1997. Postwar U.S. business cycles: An empirical investigation. Journal of Money, Credit and Banking 29, 1–16.

Johnson, S.G., 2007. The NLopt nonlinear-optimization package. `https://github.com/stevengj/nlopt`.

de Jong, R.M., Sakarya, N., 2016. The econometrics of the Hodrick-Prescott filter. The Review of Economics and Statistics 98, 310–317.

Koopman, S.J., Harvey, A., 2003. Computing observation weights for signal extraction and filtering. Journal of Economic Dynamics and Control 27, 1317–1333. doi:https://doi.org/10.1016/S0165-1889(02)00061-1.

Koopman, S.J., Shephard, N., 1992. Exact score for time series models in state space form. Biometrika 79, 823–826.

Nannicini, T., Sacchi, S., Taddei, F., 2019. The trajectory of the Jobs Act and the politics of structural reforms between counter-reforms and ambiguity. Contemporary Italian Politics 11, 310–323. doi:10.1080/23248823.2019.1643966.

OECD, 2023. OECD Employment Outlook 2023. Paris. URL: `https://www.oecd-ilibrary.org/content/publication/08785bba-en`, doi:doi:https://doi.org/10.1787/08785bba-en.

OECD, 2024. Employment rate by age group (indicator). Paris. URL: https://data.oecd.org/emp/employment-rate-by-age-group.htm, doi:doi: 10.1787/084f32c7-en.

Pelagatti, M.M., 2015. Time Series Modelling with Unobserved Components. CRC Press.

Ravn, M.O., Uhlig, H., 2002. On Adjusting the Hodrick-Prescott Filter for the Frequency of Observations. The Review of Economics and Statistics 84, 371–376. doi:10.1162/003465302317411604.

Roeger, W., Varga, J., 2008. Structural reforms in the EU: A simulation-based analysis using the QUEST model with endogenous growth. Technical Report. Directorate General Economic and Financial Affairs (DG ECFIN), European Commission.

Shibata, I., 2021. The distributional impact of recessions: The global financial crisis and the covid-19 pandemic recession. Journal of Economics and Business 115, 105971. URL: https://www.sciencedirect.com/science/article/pii/S014861952030415X, doi:https://doi.org/10.1016/j.jeconbus.2020.105971.

Svanberg, K., 2002. A class of globally convergent optimization methods based on conservative convex separable approximations. SIAM Journal on Optimization 12, 555–573. doi:10.1137/S1052623499362822.

Tito, B., 2011. Institutional reforms and dualism in European labor markets, in: Card, D., Ashenfelter, O. (Eds.), Handbook of Labor Economics. Elsevier. volume 4. chapter Chapter 13, pp. 1173–1236. doi:https://doi.org/10.1016/S0169-7218(11)02411-7.

Whittaker, E.T., 1922. On a new method of graduation. Proceedings of the Edinburgh Mathematical Society 41, 63–75. doi:10.1017/S0013091500077853.

## Appendix A. Formulae for the efficient implementation of the HP filter with jumps

We used the scalar version of the Kalman filter recursions and analytical scores of the log-likelihood function for computation speed and stability. This appendix reports all the formulae we derived and used in our R package. We share these formulae so that anybody interested in writing a similar package in other languages can easily do so.

Let us rewrite the model (1) in a slightly more general way.

$$\begin{aligned} y_t &= \alpha_t^{(1)} + \varepsilon_t, & \varepsilon_t &\sim \text{NID}(0, \sigma^2_{\varepsilon,t}) \\ \alpha_{t+1}^{(1)} &= \alpha_t^{(1)} + \alpha_t^{(2)} + \eta_t, & \eta_t &\sim \text{NID}(0, \sigma^2_{\eta,t}) \\ \alpha_{t+1}^{(2)} &= \alpha_t^{(2)} + \zeta_t, & \zeta_t &\sim \text{NID}(0, \sigma^2_{\zeta,t}) \end{aligned}$$

with initial conditions

$$\begin{bmatrix} \alpha_1^{(1)} \\ \alpha_1^{(2)} \end{bmatrix} \sim N\left( \begin{bmatrix} a_1^{(1)} \\ a_1^{(2)} \end{bmatrix}, \begin{bmatrix} p_1^{(11)} & p_1^{(12)} \\ p_1^{(12)} & p_1^{(22)} \end{bmatrix} \right)$$

*Appendix A.1. Scalar Kalman filtering recursion*

The Kalman filtering recursions, written in scalar form (to gain computational speed and insights), are as follows (for generality, we also let the measurement error variance vary over time).

The initial innovation, its variance and the Kalman gains are:

$$\begin{aligned} i_1 &= y_1 - a_1^{(1)} \\ f_1 &= p_1^{(11)} + \sigma^2_{\varepsilon,1} \\ k_1^{(1)} &= \left( p_1^{(11)} + p_1^{(12)} \right) / f_1 \\ k_1^{(2)} &= p_1^{(12)} / f_1 \end{aligned}$$

For $t = 1, 2, \ldots, n-1$ the recursions are

$$\begin{aligned} a_{t+1}^{(1)} &= a_t^{(1)} + a_t^{(2)} + k_t^{(1)} i_t \\ a_{t+1}^{(2)} &= a_t^{(2)} + k_t^{(2)} i_t \end{aligned}$$

$$\begin{aligned} p_{t+1}^{(11)} &= p_t^{(11)} + 2p_t^{(12)} + p_t^{(22)} + \sigma_{\eta,t}^2 - k_t^{(1)} k_t^{(1)} f_t \\ p_{t+1}^{(12)} &= p_t^{(12)} + p_t^{(22)} - k_t^{(1)} k_t^{(2)} f_t \\ p_{t+1}^{(22)} &= p_t^{(22)} + \sigma_{\zeta,t}^2 - k_t^{(2)} k_t^{(2)} f_t \end{aligned}$$

$$\begin{aligned} i_{t+1} &= y_{t+1} - a_{t+1}^{(1)} \\ f_{t+1} &= p_{t+1}^{11} + \sigma_{\varepsilon,t+1}^2 \\ k_{t+1}^{(1)} &= \left( p_{t+1}^{(11)} + p_{t+1}^{(12)} \right) / f_{t+1} \\ k_{t+1}^{(2)} &= p_{t+1}^{(12)} / f_{t+1} \end{aligned}$$

*Appendix A.2. Missing values treatment*

When $y_t$ is missing, four of the above equations must be modified as follows.

$$\begin{aligned} i_{t+1} &= 0 \\ f_{t+1} &= \infty \\ k_{t+1}^{(1)} &= 0 \\ k_{t+1}^{(1)} &= 0 \end{aligned}$$

*Appendix A.3. Diffuse initial conditions*

The two state variables in the state-space form are nonstationary. Unless prior information is available, their initialization should be diffuse:

$$\begin{bmatrix} \alpha_1^{(1)} \\ \alpha_1^{(2)} \end{bmatrix} \sim N \left( \begin{bmatrix} 0 \\ 0 \end{bmatrix}, \begin{bmatrix} v & 0 \\ 0 & v \end{bmatrix} \right)$$

with $v \to \infty$.

As it will be clear from the computations below when $v$ is infinite the mean squared errors of $a_t^{(1)}$ and $a_t^{(2)}$, that is, $p_1^{(11)}$ and $p_1^{(22)}$, and the variances $f_t$ of the innovations $i_t$ are infinite for $t = 1, 2$, while for $t = 3, 4, \ldots$ they are finite.

Let us compute the Kalman filter recursions for $t = 1, 2, 3$ and then take the limit for $v \to \infty$.

$t = 1$.

$$\begin{aligned}
a_1^{(1)} &= 0 \\
a_1^{(2)} &= 0 \\
p_1^{(11)} &= v \\
p_1^{(12)} &= 0 \\
p_1^{(22)} &= v \\
i_1 &= y_1 \\
f_1 &= v + \sigma^2_{\varepsilon,1} \\
k_1^{(1)} &= v/(v + \sigma^2_{\varepsilon,1}) \\
k_1^{(2)} &= 0
\end{aligned}$$

$t = 2$.

$$\begin{aligned}
a_2^{(1)} &= y_1 \\
a_2^{(2)} &= 0 \\
p_2^{(11)} &= 2v + \sigma^2_{\eta,1} - \frac{v^2}{v + \sigma^2_{\varepsilon,1}} \\
p_2^{(12)} &= v \\
p_2^{(22)} &= v + \sigma^2_{\zeta,1} \\
i_2 &= y_2 - \frac{v}{v + \sigma^2_{\varepsilon}} y_1 \to y_2 - y_1 \\
f_2 &= 2v + \sigma^2_{\eta,1} - \frac{v^2}{v + \sigma^2_{\varepsilon}} + \sigma^2_{\varepsilon,2} \\
k_2^{(1)} &= \frac{3v + \sigma^2_{\eta,1} - \frac{v^2}{v+\sigma^2_{\varepsilon,1}}}{2v + \sigma^2_{\eta,1} - \frac{v^2}{v+\sigma^2_{\varepsilon,1}} + \sigma^2_{\varepsilon,2}} \to 2 \\
k_2^{(2)} &= \frac{v}{2v + \sigma^2_{\eta,1} - \frac{v^2}{v+\sigma^2_{\varepsilon,1}} + \sigma^2_{\varepsilon,2}} \to 1
\end{aligned}$$

$t = 3$.

$$a_3^{(1)} = \frac{v^2}{v+\sigma^2_{\varepsilon,1}} y_1 + \frac{3v + \sigma^2_{\eta,1} - \frac{v^2}{v+\sigma^2_{\varepsilon,1}}}{2v + \sigma^2_{\eta,1} - \frac{v^2}{v+\sigma^2_{\varepsilon,1}} + \sigma^2_{\varepsilon,2}} \left( y_2 - \frac{v^2}{v+\sigma^2_{\varepsilon,1}} y_1 \right) \to 2y_2 - y_1$$

$$a_3^{(2)} = \frac{3v + \sigma^2_{\eta,1} - \frac{v^2}{v+\sigma^2_{\varepsilon,1}}}{2v + \sigma^2_{\eta,1} - \frac{v^2}{v+\sigma^2_{\varepsilon,1}} + \sigma^2_{\varepsilon,2}} \left( y_2 - \frac{v^2}{v+\sigma^2_{\varepsilon,1}} y_1 \right) \to y_2 - y_1$$

$$p_3^{(11)} = 5v + \sigma^2_{\eta,1} - \frac{v^2}{v+\sigma^2_{\varepsilon,1}} + \sigma^2_{\zeta,1} + \sigma^2_{\eta,2} - \frac{\left(3v + \sigma^2_{\eta,1} - \frac{v^2}{v+\sigma^2_{\varepsilon,1}}\right)^2}{2v + \sigma^2_{\eta,1} - \frac{v^2}{v+\sigma^2_{\varepsilon,1}} + \sigma^2_{\varepsilon,2}} \to \sigma^2_{\eta,1} + \sigma^2_{\eta,2} + \sigma^2_{\zeta,1}$$

$$p_3^{(12)} = 2v + \sigma^2_{\zeta,1} - \frac{v\left(3v + \sigma^2_{\eta,1} - \frac{v^2}{v+\sigma^2_{\varepsilon,1}}\right)}{2v + \sigma^2_{\eta,1} - \frac{v^2}{v+\sigma^2_{\varepsilon,1}} + \sigma^2_{\varepsilon,2}} \to \sigma^2_{\zeta,1}$$

$$p_3^{(22)} = v + \sigma^2_{\zeta,1} + \sigma^2_{\zeta,2} - \frac{v^2}{2v + \sigma^2_{\eta,1} - \frac{v^2}{v+\sigma^2_{\varepsilon,1}} + \sigma^2_{\varepsilon,2}} \to \sigma^2_{\zeta,1} + \sigma^2_{\zeta,2}$$

$$i_3 \to y_3 - 2y_2 + y_1$$
$$f_3 \to \sigma^2_{\eta,1} + \sigma^2_{\eta,2} + \sigma^2_{\zeta,1} + \sigma^2_{\varepsilon,3}$$
$$k_3^{(1)} \to \frac{\sigma^2_{\eta,1} + \sigma^2_{\eta,2} + 2\sigma^2_{\zeta,1}}{\sigma^2_{\eta,1} + \sigma^2_{\eta,2} + \sigma^2_{\zeta,1} + \sigma^2_{\varepsilon,3}}$$
$$k_3^{(2)} \to \frac{\sigma^2_{\zeta,1}}{\sigma^2_{\eta,1} + \sigma^2_{\eta,2} + \sigma^2_{\zeta,1} + \sigma^2_{\varepsilon,3}}$$

*Appendix A.4. Smoothing (Hodrick-Prescott filter)*

The smoothing recursions start from $t = n$ and work backwards to $t = 1$. The following quantities are auxiliary to compute the smoothed values of $\alpha_t^{(1)}$ and their MSE.

$$r_{n+1}^{(1)} = 0$$
$$r_{n+1}^{(2)} = 0$$
$$n_{n+1}^{(11)} = 0$$
$$n_{n+1}^{(12)} = 0$$
$$n_{n+1}^{(22)} = 0$$
$$e_n = i_n / f_n$$
$$d_n = 1 / f_n$$

For $t = n, n-1, \ldots, 1$, compute

$$
\begin{aligned}
r_t^{(1)} &= i_t/f_t + \left(1 - k_t^{(1)}\right) r_{t+1}^{(1)} - k_t^{(2)} r_{t+1}^{(2)} \\
r_t^{(2)} &= r_{t+1}^{(1)} + r_{t+1}^{(2)} \\
n_t^{(11)} &= \left(1 - k_t^{(1)}\right)^2 n_{t+1}^{(11)} - 2\left(1 - k_t^{(1)}\right) k_t^{(2)} n_{t+1}^{(12)} + k_t^{(2)} k_t^{(2)} n_{t+1}^{(22)} + 1/f_t \\
n_t^{(12)} &= \left(1 - k_t^{(1)}\right)\left(n_{t+1}^{(11)} + n_{t+1}^{(12)}\right) - k_t^{(2)}\left(n_{t+1}^{(12)} + n_{t+1}^{(22)}\right) \\
n_t^{(22)} &= n_{t+1}^{(11)} + 2n_{t+1}^{(12)} + n_{t+1}^{(22)} \\
e_{t-1} &= i_{t-1}/f_{t-1} - k_{t-1}^{(1)} r_t^{(1)} - k_{t-1}^{(2)} r_t^{(2)} \\
d_{t-1} &= 1/f_{t-1} + k_{t-1}^{(1)} k_{t-1}^{(1)} n_t^{(11)} + 2k_{t-1}^{(1)} k_{t-1}^{(2)} n_t^{(12)} + k_{t-1}^{(2)} k_{t-1}^{(2)} n_t^{(22)}
\end{aligned}
$$

The smoothed values of $\alpha_t^{(1)}$, that is, the Hodrick-Prescott filtered time series, and their mean squared errors are given by

$$
\begin{aligned}
a_{t|n}^{(1)} &= a_t^{(1)} + p_t^{(11)} r_t^{(1)} + p_t^{(12)} r_t^{(2)} \\
p_{t|n}^{(11)} &= p_t^{(11)} - p_t^{(11)} p_t^{(11)} n_t^{(11)} - 2p_t^{(11)} p_t^{(12)} n_t^{(12)} - p_t^{(12)} p_t^{(12)} n_t^{(22)}
\end{aligned}
$$

*Appendix A.5. Weights for computing the effective degrees of freedom*

Since the smoother is linear in the observations, the vector of smoothed $\alpha_t^{(1)}$, say $\hat{\boldsymbol{\mu}}$, is just a linear transformation of the vector of observations, $\boldsymbol{y}$:

$$\hat{\boldsymbol{\mu}} = \boldsymbol{S}\mathbf{y}.$$

The number of effective degrees of freedom is the trace of the weighting matrix $\boldsymbol{S}$ (Hastie et al., 2009, Section 5.4.1). The formulae for computing such weights in a general state-space form can be found in Koopman and Harvey (2003). In our framework, the diagonal elements of the matrix $\boldsymbol{S}$ are given by

$$
\begin{aligned}
s_{tt} =& p_t^{(11)}\Big(1/f_t + k_t^{(1)} k_t^{(1)} n_t^{(11)} + 2k_t^{(1)} k_t^{(2)} n_t^{(12)} \\
&+ k_t^{(2)} k_t^{(2)} n_t^{(22)} - k_t^{(1)} n_t^{(11)} - k_t^{(2)} n_t^{(12)}\Big) \\
&- p_t^{(12)}\Big(k_t^{(1)}(n_t^{(11)} + n_t^{(12)}) + k_t^{(2)}(n_t^{(12)} + n_t^{(22)})\Big)
\end{aligned}
$$

*Appendix A.6. Analytical scores*

The log-likelihood must be maximised with respect to a very large number of parameters $(n+3)$. Thus, providing the numerical optimiser with analytical scores is important for stability and speed. Since all of our parameters are related to quantities in the disturbance covariance matrices, we can adapt the results in Koopman and Shephard (1992).

Recall that our (slightly re-parametrised) model is

$$\begin{aligned} y_t &= \alpha_t^{(1)} + \varepsilon_t, & \varepsilon_t &\sim \mathrm{NID}(0, \sigma_\varepsilon^2) \\ \alpha_{t+1}^{(1)} &= \alpha_t^{(1)} + \alpha_t^{(2)} + \eta_t, & \eta_t &\sim \mathrm{NID}(0, \sigma_t^2) \\ \alpha_{t+1}^{(2)} &= \alpha_t^{(2)} + \zeta_t, & \zeta_t &\sim \mathrm{NID}(0, \sigma^2 + \gamma^2 \sigma_t^2) \end{aligned}$$

where the parameters to estimate are $\sigma_\varepsilon$, $\sigma$, $\gamma$, and the sequence $\{\sigma_t\}_{t=1,\dots,n}$, which are all non-negative. Notice that in this parametrisation $\lambda = \sigma_\varepsilon^2/\sigma^2$.

*$\lambda$ not fixed.* If $\lambda$ is not fixed and $\ell(\boldsymbol{\theta})$ represents the log-likelihood function, with $\boldsymbol{\theta}$ vector all of the parameters, then

$$\begin{aligned} \frac{\partial \ell}{\partial \sigma_\varepsilon} &= \sigma_\varepsilon \sum_{t=1}^{n} (e_t e_t - d_t) \\ \frac{\partial \ell}{\partial \sigma} &= \sigma \sum_{t=1}^{n} (r_t^{(2)} r_t^{(2)} - n_t^{(22)}) \\ \frac{\partial \ell}{\partial \gamma} &= \gamma \sum_{t=1}^{n} (r_t^{(2)} r_t^{(2)} - n_t^{(22)}) \sigma_t^2 \\ \frac{\partial \ell}{\partial \sigma_t} &= \Big( r_t^{(1)} r_t^{(1)} - n_t^{(11)} + (r_t^{(2)} r_t^{(2)} - n_t^{(22)}) \gamma^2 \Big) \sigma_t^2 \end{aligned}$$

Generally, constrained optimisation problems also need the derivatives of the constraining function, which in our case is $g(\boldsymbol{\theta}) = \sum_{t=1}^{n} \sigma_t$. The solution to the regularised maximum likelihood problem must satisfy $g(\boldsymbol{\theta}) \leq M$. The derivatives are trivial:

$$\frac{\partial g}{\sigma_\varepsilon} = 0, \ \frac{\partial g}{\sigma} = 0, \ \frac{\partial g}{\gamma} = 0, \ \frac{\partial g}{\sigma_t} = 1.$$

$\lambda$ *fixed.* If $\lambda$ is fixed, $\sigma_\varepsilon^2 = \lambda\sigma^2$ and, in the log-likelihood function $\ell(\boldsymbol{\theta})$, the vector of parameters $\boldsymbol{\theta}$ does not contain $\lambda$ or $\sigma_\varepsilon^2$. The derivatives are now

$$\begin{aligned}
\frac{\partial \ell}{\partial \sigma} &= \sigma \sum_{t=1}^{n} (r_t^{(2)} r_t^{(2)} - n_t^{(22)}) - \sigma\lambda \sum_{t=1}^{n} (e_t e_t - d_t) \\
\frac{\partial \ell}{\partial \gamma} &= \gamma \sum_{t=1}^{n} (r_t^{(2)} r_t^{(2)} - n_t^{(22)}) \sigma_t \\
\frac{\partial \ell}{\partial \sigma_t} &= \Big( r_t^{(1)} r_t^{(1)} - n_t^{(11)} + (r_t^{(2)} r_t^{(2)} - n_t^{(22)}) \gamma^2 \Big) \sigma_t^2
\end{aligned}$$

The derivatives of the constraining function are

$$\frac{\partial g}{\sigma} = 0, \ \frac{\partial g}{\gamma} = 0, \ \frac{\partial g}{\sigma_t} = 1.$$

# Supplementary Materials to
## A Hodrick-Prescott filter with automatically selected jumps

Paolo Maranzano[a,b], Matteo Pelagatti[a]

[a]*Department of Economics, Management and Statistics, University of Milano-Bicocca, Via Bicocca degli Arcimboldi, 8, Milano, 20126, MI, Italy*
[b]*Fondazione Eni Enrico Mattei, C.so Magenta, 63, Milano, 20123, MI, Italy*

---

---

*Email addresses:* paolo.maranzano@unimib.it (Paolo Maranzano), matteo.pelagatti@unimib.it (Matteo Pelagatti)

*Preprint submitted to Elsevier* *July 3, 2024*

# 1. Extended results for Section "Assessing structural breaks in the Italian labour market"

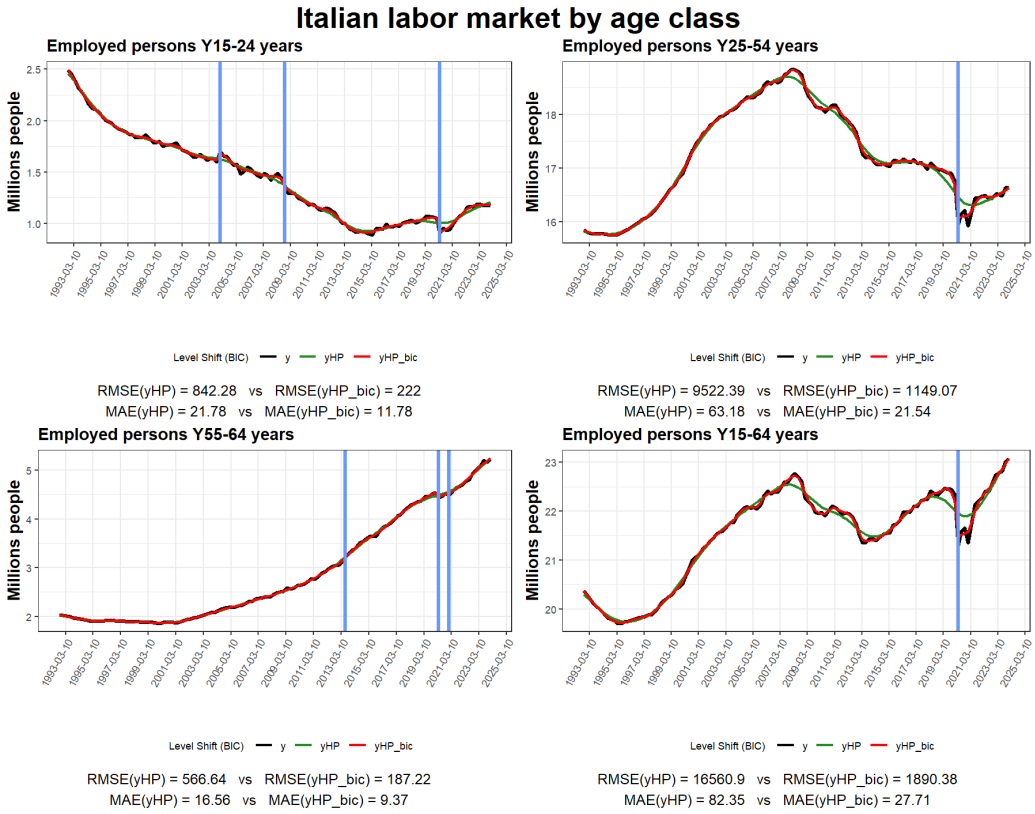


Figure 1: Actual and smoothed time series for employed persons in Italy by age class. Black curves represent the raw data; the vertical lines represent the structural breaks identified by the HPJ using the BIC; Green curves (yHP) are the smoothed values using the standard HP filter; red curves (yHP_bic) are the smoothed values produced by the HP filter with jumps. Under each subplot, we report the two smoothers' Root Mean Squared Error (RMSE) and Mean Absolute Error (MAE).

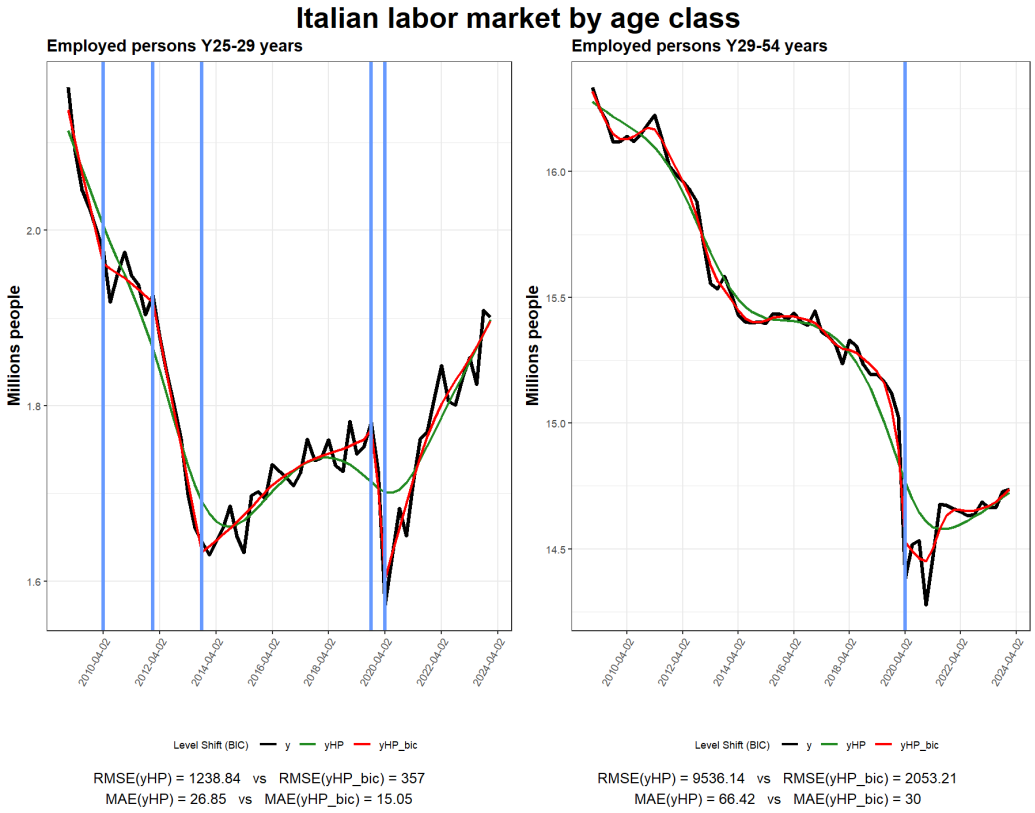


Figure 2: Actual and smoothed time series series for employed persons (million people) in Italy by age class (2009Q1-2023Q4). Black curves represent early-career (left) and experienced workers (right). Light blue vertical lines represent the structural breaks identified by the HPJ algorithm through the BIC. Green curves (yHP) are the smoothed values using the basic HP filter, whereas red curves (yHP_bic) are the smoothed values produced by the HP jumps filter. Under each subplot, we report the Root Mean Squared Error (RMSE) and Mean Absolute Error (MAE) without jumps allowed (yHP) and with jump allowed (yHP_bic).

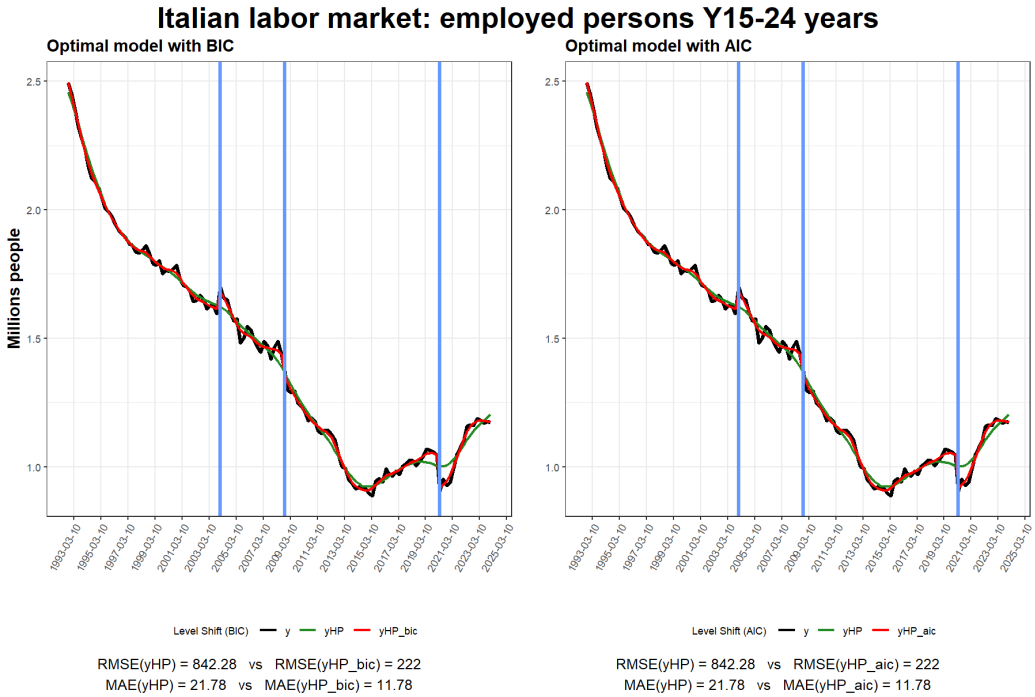


Figure 3: Actual and smoothed time series for Italian employed persons (millions) with ages from 15 to 24 years (1993Q1-2023Q4). Black curves represent the actual time series, while green curves (yHP) are the smoothed values using the basic HP filter and red curves (yHP_bic) are the smoothed values produced by the HP jumps filter. Light blue vertical lines represent the structural breaks identified by the HPJ algorithm through the BIC (left) and the AIC criteria (right). Under each subplot, we report the Root Mean Squared Error (RMSE) and Mean Absolute Error (MAE) without jumps allowed (yHP) and with jump allowed (yHP_bic).

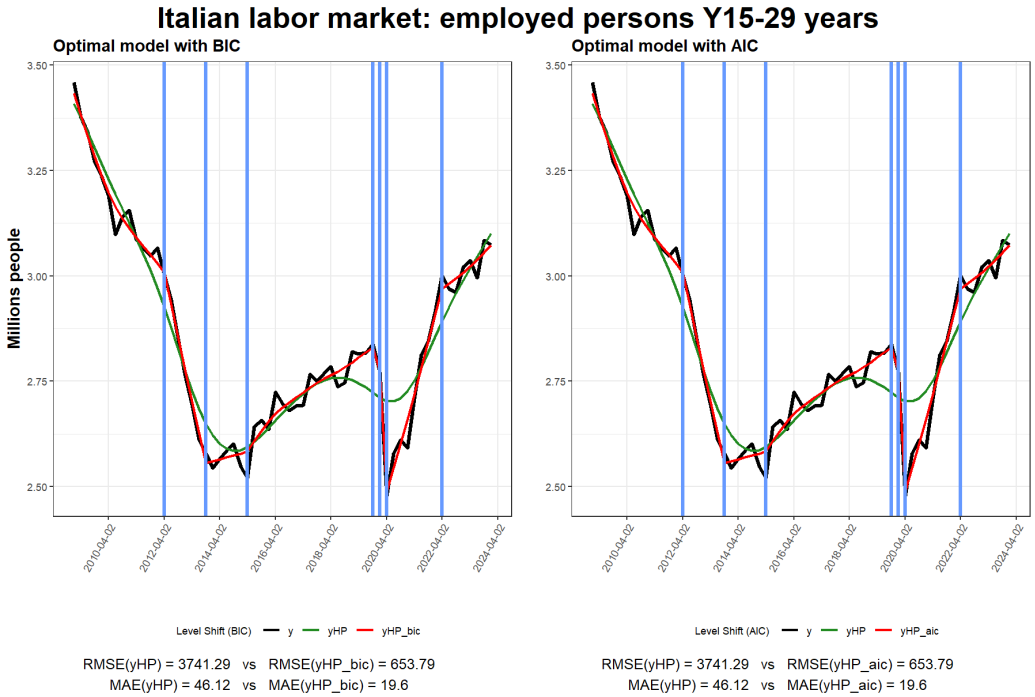


Figure 4: Actual and smoothed time series for Italian employed persons (millions) with ages from 15 to 29 years (2009Q1-2023Q4). Black curves represent the actual time series, while green curves (yHP) are the smoothed values using the basic HP filter and red curves (yHP_bic) are the smoothed values produced by the HP jumps filter. Light blue vertical lines represent the structural breaks identified by the HPJ algorithm through the BIC (left) and the AIC criteria (right). Under each subplot, we report the Root Mean Squared Error (RMSE) and Mean Absolute Error (MAE) without jumps allowed (yHP) and with jump allowed (yHP_bic).

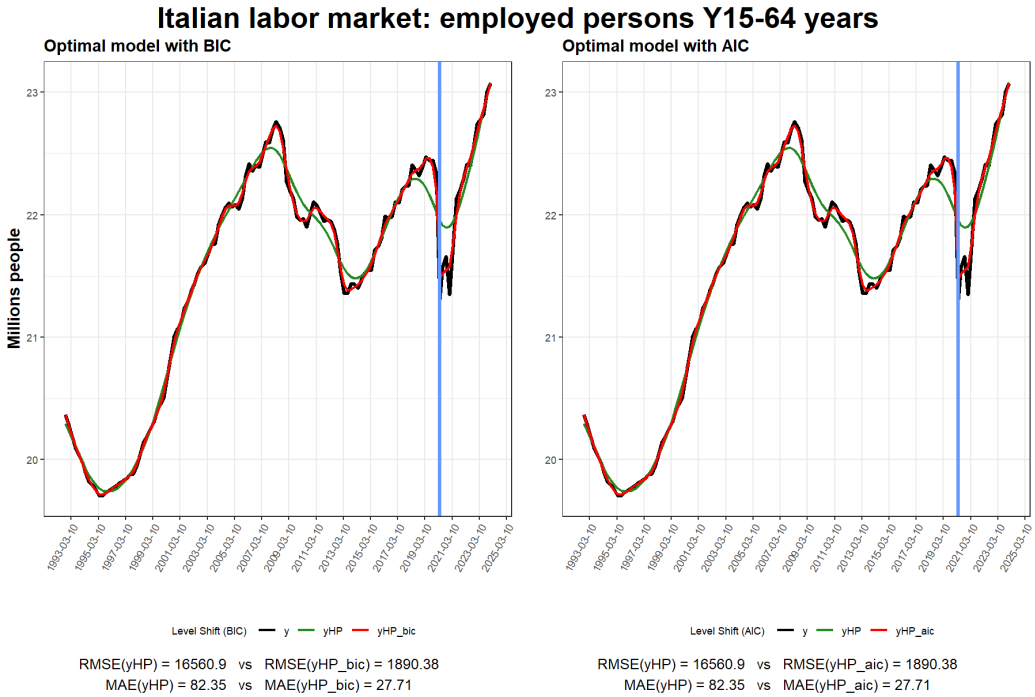


Figure 5: Actual and smoothed time series for Italian employed persons (millions) with ages from 15 to 64 years (1993Q1-2023Q4). Black curves represent the actual time series, while green curves (yHP) are the smoothed values using the basic HP filter and red curves (yHP_bic) are the smoothed values produced by the HP jumps filter. Light blue vertical lines represent the structural breaks identified by the HPJ algorithm through the BIC (left) and the AIC criteria (right). Under each subplot, we report the Root Mean Squared Error (RMSE) and Mean Absolute Error (MAE) without jumps allowed (yHP) and with jump allowed (yHP_bic).

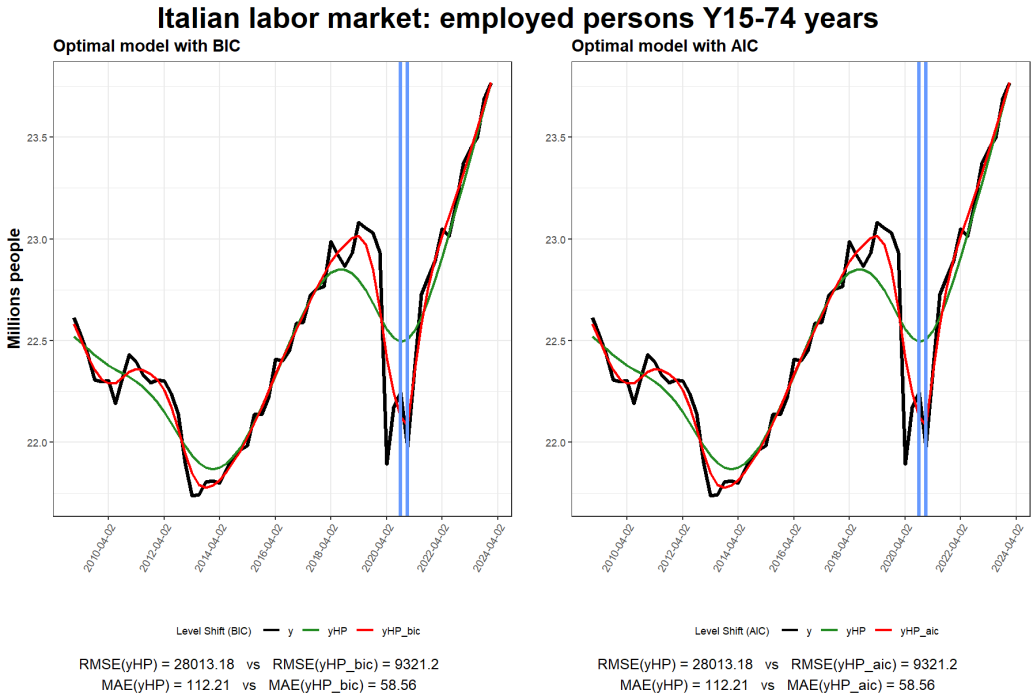


Figure 6: Actual and smoothed time series for Italian employed persons (millions) with ages from 15 to 74 years (2009Q1-2023Q4). Black curves represent the actual time series, while green curves (yHP) are the smoothed values using the basic HP filter and red curves (yHP_bic) are the smoothed values produced by the HP jumps filter. Light blue vertical lines represent the structural breaks identified by the HPJ algorithm through the BIC (left) and the AIC criteria (right). Under each subplot, we report the Root Mean Squared Error (RMSE) and Mean Absolute Error (MAE) without jumps allowed (yHP) and with jump allowed (yHP_bic).

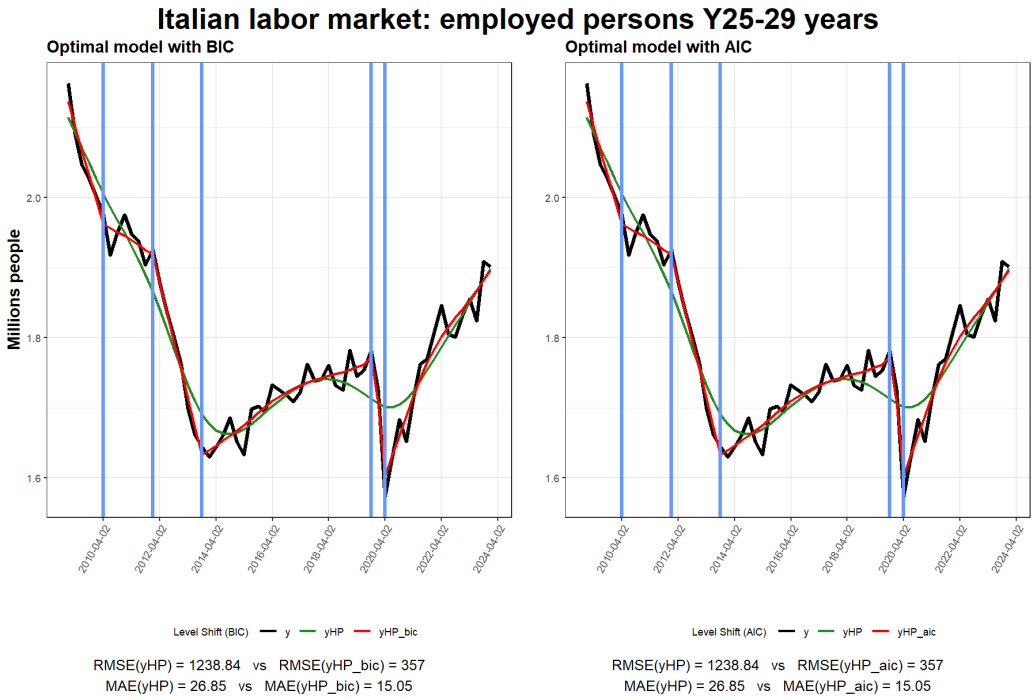


Figure 7: Actual and smoothed time series for Italian employed persons (millions) with ages from 25 to 29 years (2009Q1-2023Q4). Black curves represent the actual time series, while green curves (yHP) are the smoothed values using the basic HP filter and red curves (yHP_bic) are the smoothed values produced by the HP jumps filter. Light blue vertical lines represent the structural breaks identified by the HPJ algorithm through the BIC (left) and the AIC criteria (right). Under each subplot, we report the Root Mean Squared Error (RMSE) and Mean Absolute Error (MAE) without jumps allowed (yHP) and with jump allowed (yHP_bic).

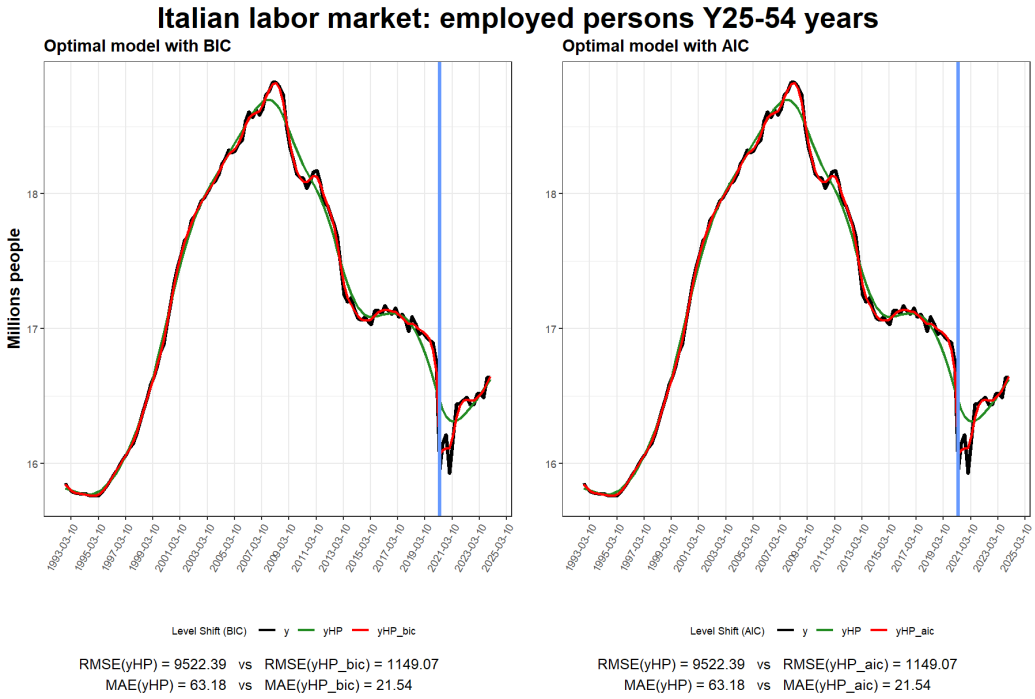


Figure 8: Actual and smoothed time series for Italian employed persons (millions) with ages from 25 to 54 years (1993Q1-2023Q4). Black curves represent the actual time series, while green curves (yHP) are the smoothed values using the basic HP filter and red curves (yHP_bic) are the smoothed values produced by the HP jumps filter. Light blue vertical lines represent the structural breaks identified by the HPJ algorithm through the BIC (left) and the AIC criteria (right). Under each subplot, we report the Root Mean Squared Error (RMSE) and Mean Absolute Error (MAE) without jumps allowed (yHP) and with jump allowed (yHP_bic).

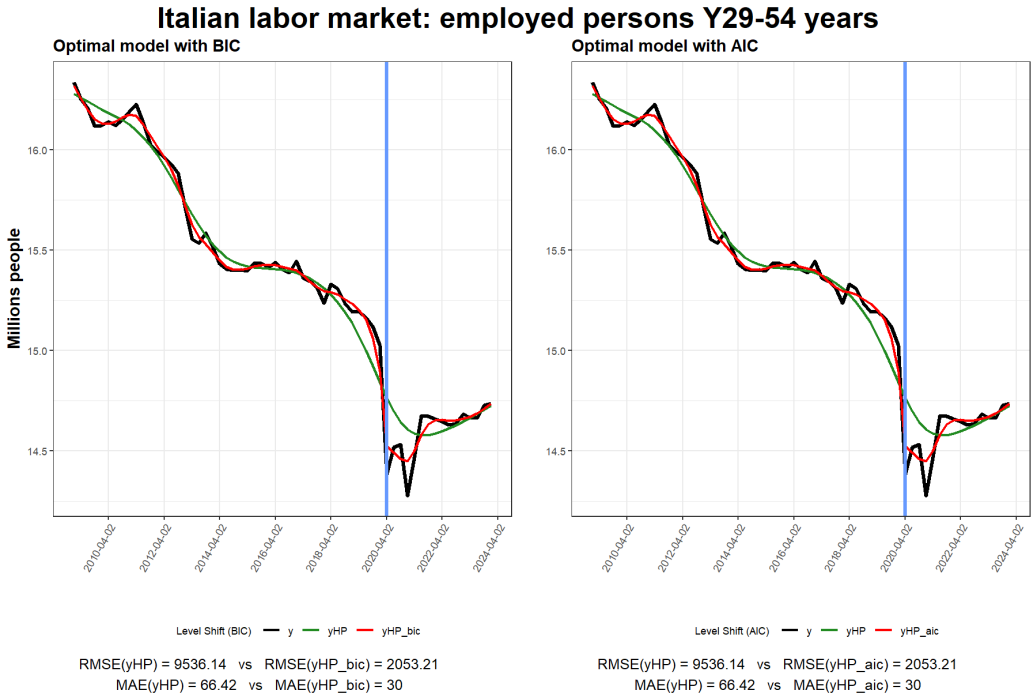


Figure 9: Actual and smoothed time series for Italian employed persons (millions) with ages from 29 to 54 years (2009Q1-2023Q4). Black curves represent the actual time series, while green curves (yHP) are the smoothed values using the basic HP filter and red curves (yHP_bic) are the smoothed values produced by the HP jumps filter. Light blue vertical lines represent the structural breaks identified by the HPJ algorithm through the BIC (left) and the AIC criteria (right). Under each subplot, we report the Root Mean Squared Error (RMSE) and Mean Absolute Error (MAE) without jumps allowed (yHP) and with jump allowed (yHP_bic).

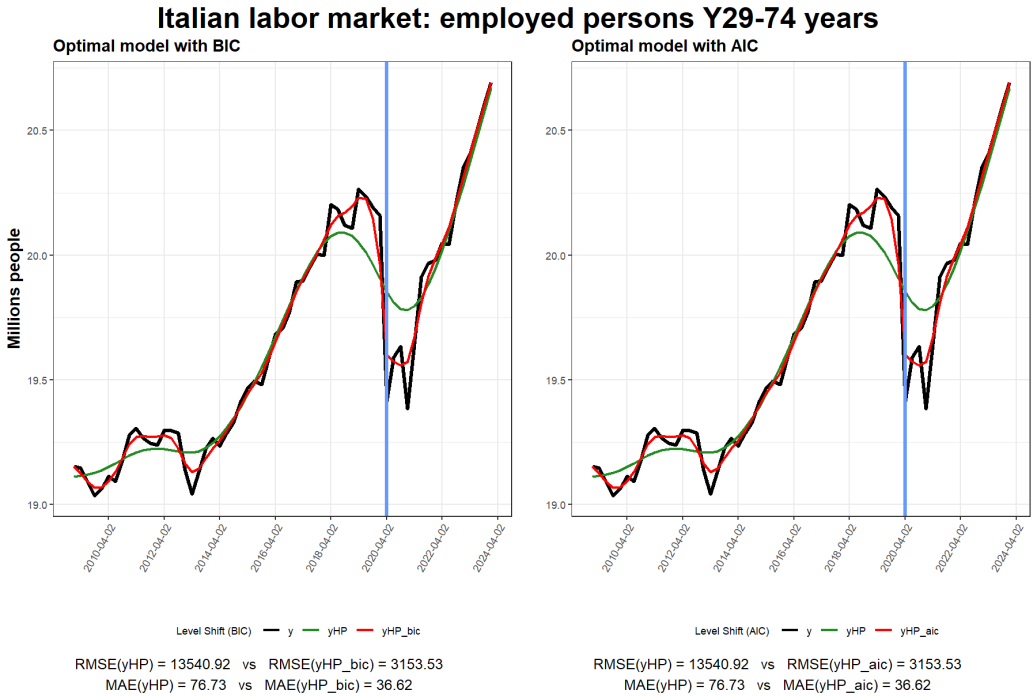


Figure 10: Actual and smoothed time series for Italian employed persons (millions) with ages from 29 to 74 years (2009Q1-2023Q4). Black curves represent the actual time series, while green curves (yHP) are the smoothed values using the basic HP filter and red curves (yHP_bic) are the smoothed values produced by the HP jumps filter. Light blue vertical lines represent the structural breaks identified by the HPJ algorithm through the BIC (left) and the AIC criteria (right). Under each subplot, we report the Root Mean Squared Error (RMSE) and Mean Absolute Error (MAE) without jumps allowed (yHP) and with jump allowed (yHP_bic).

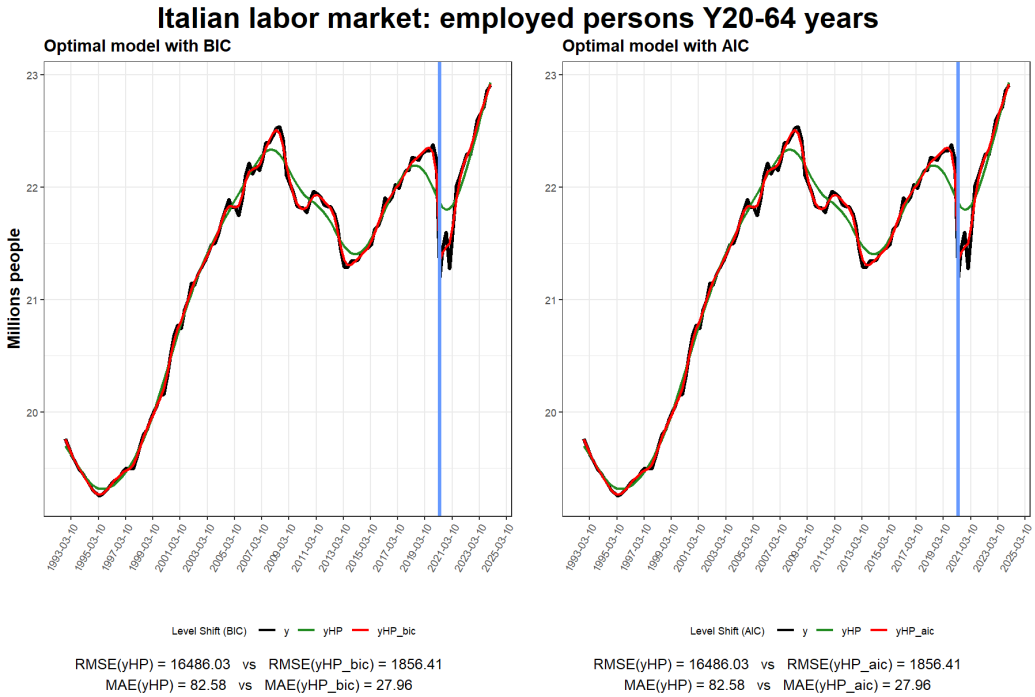


Figure 11: Actual and smoothed time series for Italian employed persons (millions) with ages from 20 to 64 years (1993Q1-2023Q4). Black curves represent the actual time series, while green curves (yHP) are the smoothed values using the basic HP filter and red curves (yHP_bic) are the smoothed values produced by the HP jumps filter. Light blue vertical lines represent the structural breaks identified by the HPJ algorithm through the BIC (left) and the AIC criteria (right). Under each subplot, we report the Root Mean Squared Error (RMSE) and Mean Absolute Error (MAE) without jumps allowed (yHP) and with jump allowed (yHP_bic).

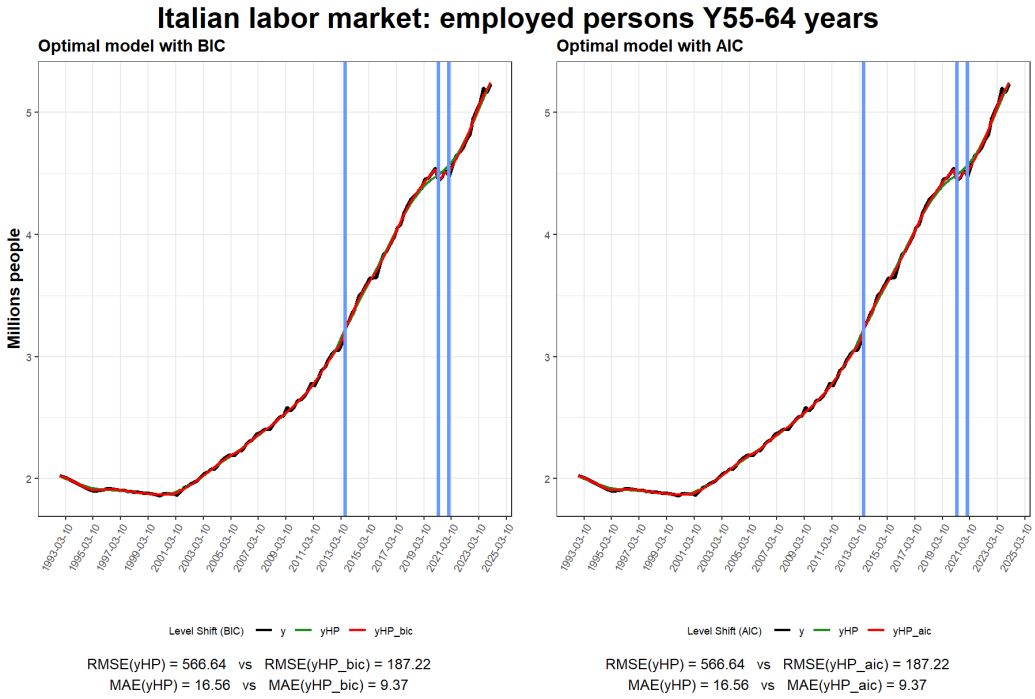


Figure 12: Actual and smoothed time series for Italian employed persons (millions) with ages from 55 to 64 years (1993Q1-2023Q4). Black curves represent the actual time series, while green curves (yHP) are the smoothed values using the basic HP filter and red curves (yHP_bic) are the smoothed values produced by the HP jumps filter. Light blue vertical lines represent the structural breaks identified by the HPJ algorithm through the BIC (left) and the AIC criteria (right). Under each subplot, we report the Root Mean Squared Error (RMSE) and Mean Absolute Error (MAE) without jumps allowed (yHP) and with jump allowed (yHP_bic).

FONDAZIONE ENI ENRICO MATTEI WORKING PAPER SERIES

Our Working Papers are available on the Internet at the following address:
https://www.feem.it/pubblicazioni/feem-working-papers/

## "NOTE DI LAVORO" PUBLISHED IN 2024

1. A. Sileo, M. Bonacina, The automotive industry: when regulated supply fails to meet demand. The Case of Italy
2. A. Bastianin, E. Mirto, Y. Qin, L. Rossini, What drives the European carbon market? Macroeconomic factors and forecasts
3. M. Rizzati, E. Ciola, E. Turco, D. Bazzana, S. Vergalli, Beyond Green Preferences: Alternative Pathways to Net-Zero Emissions in the MATRIX model
4. L. Di Corato, M. Moretto, Supply contracting under dynamic asymmetric cost information
5. C. Drago, L. Errichiello, Remote work admist the Covid-19 outbreak: Insights from an Ensemble Community-Based Keyword Network Analysis
6. F. Cappelli, Unequal contributions to CO2 emissions along the income distribution within and between countries
7. I. Bos, G. Maccarrone, M. A. Marini, Anti-Consumerism: Stick or Carrot?
8. M. Gilli, A. Sorrentino, The Set of Equilibria in Max-Min Two Groups Contests with Binary Actions and a Private Good Prize
9. E. Bachiocchi, A. Bastianin, G. Moramarco, Macroeconomic Spillovers of Weather Shocks across U.S. States
10. T. Schmitz, I. Colantone, G. Ottaviano, Regional and Aggregate Economic Consequences of Environmental Policy
11. D. Bosco, M. Gilli, Effort Provision and Incentivisation in Tullock Group-Contests with Many Groups: An Explicit Characterisation
12. A. Drigo, Environmental justice gap in Italy: the role of industrial agglomerations and regional pollution dispersion capacity
13. P. I. Rivadeneyra García, F. Cornacchia, A. G. Martínez Hernández, M. Bidoia, C. Giupponi, Multi-platform assessment of coastal protection and carbon sequestration in the Venice Lagoon under future scenarios
14. T. Angel, A. Berthe, V. Costantini, M. D'Angeli, How the nature of inequality reduction matters for CO2 emissions
15. E. Bacchiocchi, A. Bastianin, T. Kitagawa, E. Mirto, Partially identified heteroskedastic SVARs
16. B. Bosco, C. F. Bosco, P. Maranzano, Income taxation and labour response. Empirical evidence from a DID analysis of an income tax treatment in Italy
17. M. M. H. Sarker, A. Gabino Martinez-Hernandez, J. Reyes Vásquez, P. Rivadeneyra, S. Raimondo, Coastal Infrastructure and Climate Change adaptation in Bangladesh: Ecosystem services insights from an integrated SES-DAPSIR framework

**Fondazione Eni Enrico Mattei**
Corso Magenta 63, Milano – Italia

Tel. +39 02 403 36934

E-mail: letter@feem.it
**www.feem.it**

Fondazione Eni Enrico Mattei